Cell Reports
Medicine

Article

Pulmonary MTBVAC vaccination induces immune signatures previously correlated with prevention of tuberculosis infection

Graphical Abstract

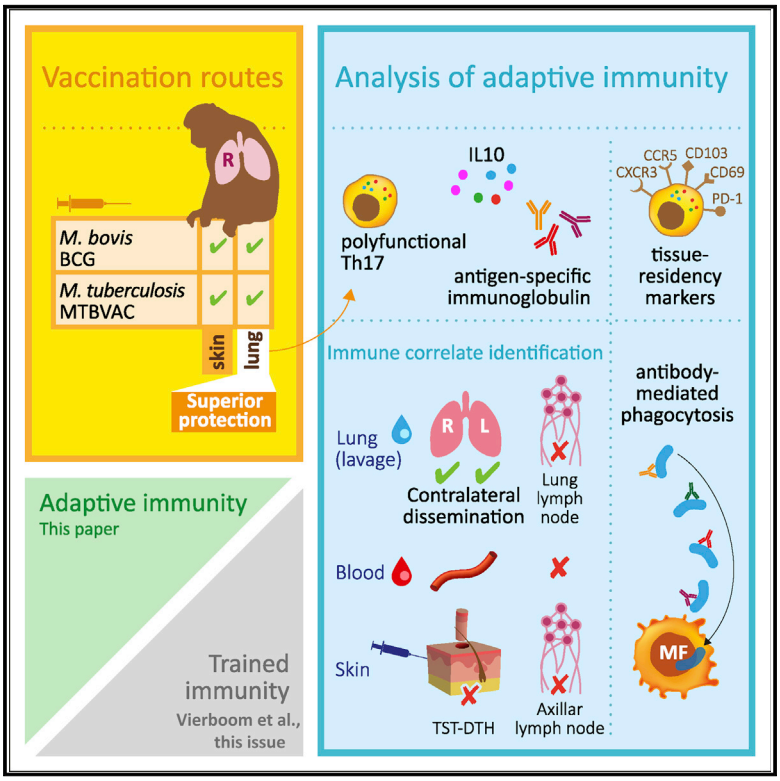

Highlights

- Pulmonary MTBVAC delivery confers immune signature correlating with TB protection
- This signature spreads through the lung without a recall response in the skin
- Vaccine-induced T cells have increased mucosal homing and tissue residency markers
- Vaccine-induced antibodies enhance phagocytosis of *M. tuberculosis*

Authors

Karin Dijkman, Nacho Aguilo, Charelle Boot, ..., Eugenia Puentes, Carlos Martin, Frank A.W. Verreck

Correspondence

verreck@bprc.nl

In Brief

Dijkman et al. show that pulmonary immunization with the *M. tuberculosis*-derived vaccine candidate MTBVAC confers a local mucosal antigen-specific signature—polyfunctional Th1/Th17 cells exhibiting increased homing and tissue residency marker expression, IL-10, and phagocytosis-promoting immunoglobulins—that has been associated previously with protection from TB infection and disease in rhesus macaques.

Dijkman et al., 2021, Cell Reports Medicine *2*, 100187
January 19, 2021
https://doi.org/10.1016/j.xcrm.2020.100187

CellPress

Cell Reports Medicine

CellPress
OPEN ACCESS

Article

Pulmonary MTBVAC vaccination induces immune signatures previously correlated with prevention of tuberculosis infection

Karin Dijkman,[1] Nacho Aguilo,[2,3] Charelle Boot,[1] Sam O. Hofman,[1] Claudia C. Sombroek,[1] Richard A.W. Vervenne,[1] Clemens H.M. Kocken,[1] Dessislava Marinova,[2,3] Jelle Thole,[4] Esteban Rodríguez,[5] Michel P.M. Vierboom,[1] Krista G. Haanstra,[1] Eugenia Puentes,[5] Carlos Martin,[2,3] and Frank A.W. Verreck[1,6,*]

[1]Biomedical Primate Research Centre (BPRC), Rijswijk, the Netherlands
[2]Department of Microbiology, Faculty of Medicine, IIS Aragon, University of Zaragoza, Zaragoza, Spain
[3]CIBERES, Instituto de Salud Carlos III, Madrid, Spain
[4]TuBerculosis Vaccine Initiative (TBVI), Lelystad, the Netherlands
[5]Biofabri, Pontevedra, Spain
[6]Lead contact
*Correspondence: verreck@bprc.nl
https://doi.org/10.1016/j.xcrm.2020.100187

SUMMARY

To fight tuberculosis, better vaccination strategies are needed. Live attenuated *Mycobacterium tuberculosis*-derived vaccine, MTBVAC, is a promising candidate in the pipeline, proven to be safe and immunogenic in humans so far. Independent studies have shown that pulmonary mucosal delivery of Bacillus Calmette-Guérin (BCG), the only tuberculosis (TB) vaccine available today, confers superior protection over standard intradermal immunization. Here we demonstrate that mucosal MTBVAC is well tolerated, eliciting polyfunctional T helper type 17 cells, interleukin-10, and immunoglobulins in the airway and yielding a broader antigenic profile than BCG in rhesus macaques. Beyond our previous work, we show that local immunoglobulins, induced by MTBVAC and BCG, bind to *M. tuberculosis* and enhance pathogen uptake. Furthermore, after pulmonary vaccination, but not *M. tuberculosis* infection, local T cells expressed high levels of mucosal homing and tissue residency markers. Our data show that pulmonary MTBVAC administration has the potential to enhance its efficacy and justifies further exploration of mucosal vaccination strategies in preclinical efficacy studies.

INTRODUCTION

Despite advances in treatment and care, tuberculosis continues to cause approximately 1.6 million deaths and an additional 10 million cases of active disease annually.[1] Control of this ongoing epidemic is complicated by a lack of accurate diagnostics, lengthy treatment regimens, and an increase in drug-resistant tuberculosis (TB) incidence. An effective vaccination strategy preventing TB infection or disease is therefore of critical importance for controlling the continuing TB epidemic. Unfortunately, the only prophylactic vaccine currently available, Bacillus Calmette-Guérin (BCG), despite preventing dissemination of the disease, is notoriously variable in protecting adults and adolescents from pulmonary TB. Pulmonary disease is the major cause of morbidity and mortality and the driver of TB spread.[2] Geographical location, prior non-tuberculous mycobacterium (NTM) exposure, and over-attenuation of BCG have been implied in the variable BCG efficacy.[2–4] Regardless of the underlying mechanisms of this variation in efficacy, it is evident that a more reliable vaccine strategy is urgently needed.

Currently, multiple novel TB vaccines are being developed to replace BCG at birth or to serve as a (heterologous) booster on top of prior BCG vaccination.[5,6] One of these new candidate vaccines is MTBVAC, a live attenuated whole-cell vaccine designed as a potential replacement for neonatal BCG vaccination. MTBVAC was generated by genetic modification of a clinical *Mycobacterium tuberculosis* (*Mtb*) isolate of the lineage 4 Euro-American genotype and harbors deletions in two virulence genes, *phoP* and *fadD26*.[7,8] These deletions interfere with transcription, synthesis, and/or secretion of multiple virulence factors, including early secretory antigenic target 6 (ESAT6) and phthiocerol dimycocerosates (PDIMs).[9] Because MTBVAC is *Mtb* derived, it contains genomic regions of difference (RDs) that are absent from *M. bovis*, and in particular also RD1, that is lacking from *M. bovis*-derived BCG.[9] MTBVAC, therefore, has a broader antigenic repertoire that is linked to its enhanced protective capacity.[10] Although RD1 encodes notorious virulence factors, such as ESAT6, secretion is tightly regulated and interrupted by the targeted *phoP* deletion in MTBVAC.[9] Accordingly, in early-stage clinical evaluation in adults and infants, intradermal MTBVAC immunization has been found to have an acceptable safety profile comparable with BCG, corroborating its attenuated phenotype.[11,12]

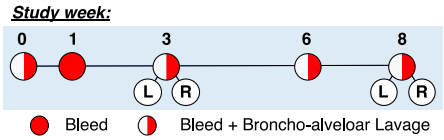

Route of vaccination	BCG	MTBVAC
Intradermal	B.id	M.id
Pulmonary mucosal	B.muc	M.muc

Figure 1. Study design schematic

Shown is a schematic overview of vaccination strategies and post-vaccination sampling (of peripheral blood and BAL). Of note, BALs were harvested bilaterally only for the mucosally vaccinated groups 3 and 8 weeks after vaccination.

In preclinical studies MTBVAC presented with an ability to protect from experimental TB infection and disease better than BCG.[7,13] It has been shown to confer improved protective efficacy against *Mtb* in newborn mice at a single dose at birth.[13] In guinea pigs, revaccination with MTBVAC after BCG priming resulted in a further reduction of *Mtb* burden in the lung compared with BCG alone,[14] and non-human primate data on the efficacy of (re)vaccination with intradermal MTBVAC have been established recently.[15] Although initially designed as a vaccine for newborns, MTBVAC is also considered for revaccination of BCG-primed adolescents and adults.[12] Phase2 dose-finding, safety, and immunogenicity studies in neonates (NCT03536117) and QuantiFERON-negative and -positive adults (NCT02933281) are in progress, and a subsequent phase 3 efficacy study in neonates is scheduled to start in 2021.

The indicated route of administration for BCG and MTBVAC is the skin, which induces limited immune responses at the pulmonary mucosa, the primary site of infection with *Mtb*. A growing body of data generated in preclinical models of TB shows that altering the route of BCG administration to the pulmonary mucosa significantly improves its protective efficacy.[16–19] In previous work, we showed that pulmonary but not intradermal BCG vaccination could protect highly susceptible rhesus macaques (*Macaca mulatta*) from repeated low-dose *Mtb* infection and TB-associated pathology.[20] Macaques are considered to be a predictive model for TB vaccine development because of their close phylogenetic relationship to man and highly similar TB disease development.[21,22] In this model, the protection conferred by mucosal BCG statistically correlated with induction of polyfunctional interleukin-17A (IL-17A)+ CD4+ T cells at the pulmonary mucosa and IL-10 production by bronchoalveolar lavage (BAL) cells, whereas elevated levels of antigen-specific immunoglobulins were found in association with mucosal BCG immunization as well.

Although the mucosa of the airways can be considered an environment of robust innate host defense to warrant homeostatic balance, potentially resulting in rapid clearance and poor immunogenicity of live attenuated vaccines, our data from mucosal delivery in non-human primates (NHPs) have shown local persistence of BCG and protection-associated immunity in the airways in the absence of overt respiratory adversity.[20] Interestingly, on this note, prior exposure of BCG to alveolar lining fluid from naive animals *in vitro* has been described to enhance its protective efficacy when administered peripherally to mice.[23] Also, in other NHP studies exploring pulmonary delivery of BCG, no adversity has been reported.[24,25] However, for pulmonary mucosal delivery of MTBVAC, the tolerability and immunogenicity remain to be established.

In light of this, here we set out to assess the tolerability and immunogenicity of pulmonary mucosal delivery of MTBVAC in rhesus macaques. Using a two-by-two factorial design strategy, we compared MTBVAC with BCG by standard intradermal injection and endobronchial instillation of a standard human dose. Corroborating our earlier observations regarding alternative BCG delivery, we show that pulmonary MTBVAC administration was well tolerated and induced local IL-17A-producing T cells, IL-10 production, and *Mtb*-specific immunoglobulin A (IgA). Compared with BCG, vaccination with MTBVAC resulted in more rapid induction of immune responses and broader antigenic specificity. Beyond what we have reported previously for mucosal BCG, we identified increased expression of mucosal homing markers of purified protein derivative (PPD)-specific T cells in lung wash samples of mucosally vaccinated but not *Mtb*-infected animals. Furthermore, we show that vaccine-induced mucosal antibodies are functional in binding to live *Mtb* and facilitating pathogen uptake by phagocytes. In our attempt to identify an immune correlate of pulmonary whole-cell TB vaccination that is assessable by peripheral sampling, we exploited *in vivo* recall stimulation by tuberculin skin testing (TST) but could not identify meaningful responses in skin or skin-draining axillary lymph nodes. This study corroborates and extends beyond previous findings and provides a rationale for future exploration of mucosal administration of MTBVAC with the perspective of improving our prophylaxis against TB infection and disease.

RESULTS

Local immune signatures after mucosal MTBVAC vaccination

To interrogate whether the *Mtb*-derived MTBVAC vaccine candidate, like *M. bovis* BCG, is tolerated well and induces unique immune features upon pulmonary mucosal administration, we designed a dedicated safety/immunogenicity study (without infectious challenge) in rhesus macaques, represented schematically in Figure 1. We vaccinated with MTBVAC using a single (human) dose similar to BCG (5×10^5 colony-forming units [CFUs]/dose) through the standard intradermal route (M.id) or endobronchial instillation (M.muc) for direct comparison with intradermal or mucosal BCG vaccination (B.id and B.muc, respectively; Figure 1).

On a daily basis, animals were monitored for changes in condition and well-being (including but not limited to alertness, appetite, and respiration), but no deviation from normal behavior was observed that would indicate vaccine adversity. Moreover, there were no signals of serological increase in C-reactive protein (CRP) levels during the study that would indicate an adverse systemic inflammatory response related to treatment (Figure S1). Although we aimed to address vaccine persistence by culturing from lung wash samples, our effort failed because of technical error; therefore we could not confirm persistence of MTBVAC in the airway like we have shown previously for BCG.[20] In

CellPress
OPEN ACCESS

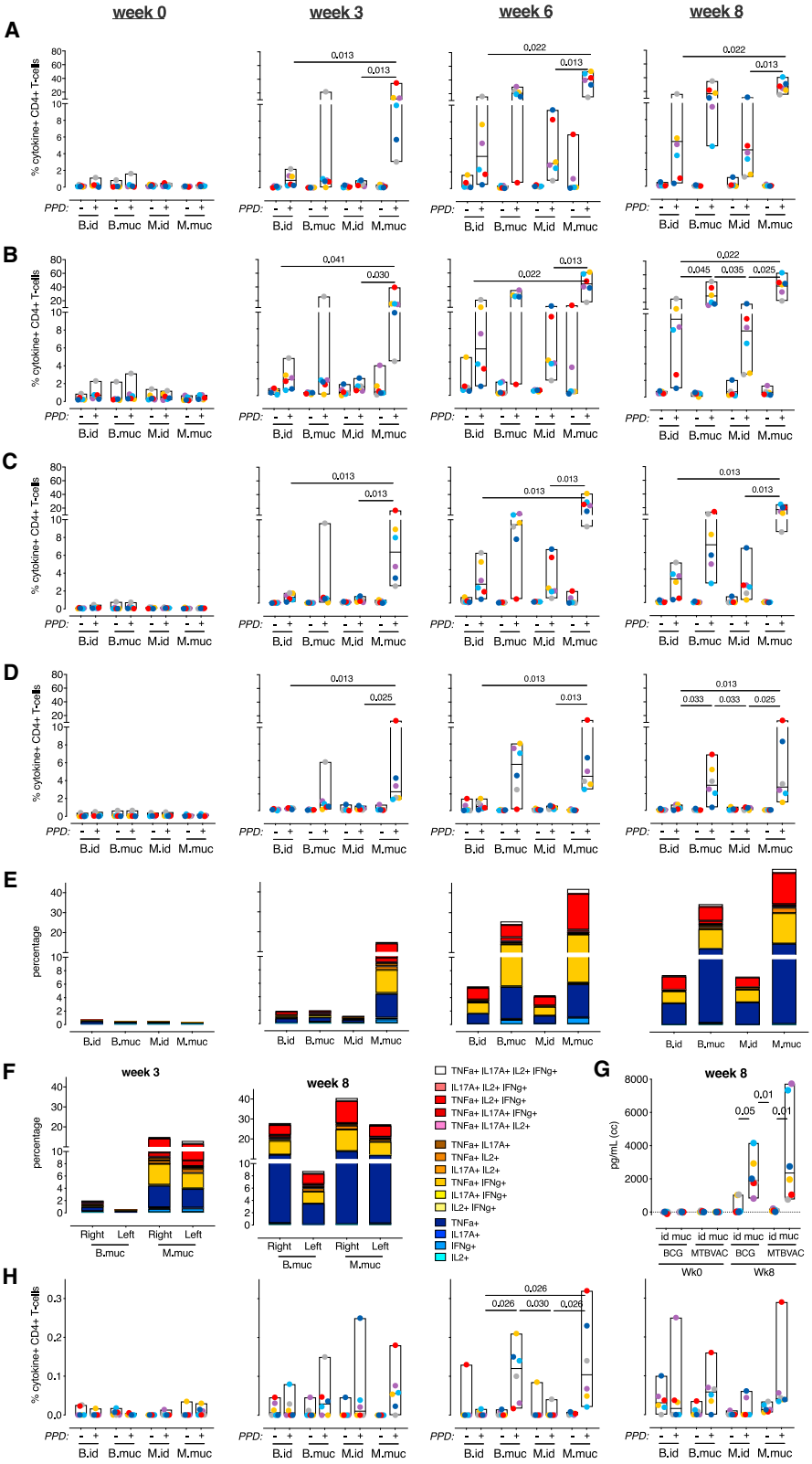

(legend on next page)

summary, and within limits of observation, live attenuated *Mtb*-derived MTBVAC, also by pulmonary mucosal delivery, was well tolerated by rhesus macaques.

Flow cytometry profiling of T cells in BAL revealed robust induction of PPD-specific CD4+ T cells in both mucosally vaccinated groups, with MTBVAC eliciting higher responses than BCG for almost all cytokines, especially early after vaccination (Figures 2A–2D). Although intradermal BCG and MTBVAC showed an increase in interferon γ (IFNγ)-, tumor necrosis factor alpha (TNF-α)-, and IL-2-producing T cells in the airways in the weeks following vaccination (Figures 2A–2C), IL-17A production was uniquely observed in the mucosally vaccinated groups (Figure 2D). These IL-17A+ T cells also produced IFNγ, TNF-α, and IL-2, confirming induction of a local, quadruple-positive, CD4+ T cell population (Figure 2E), found previously to be associated in this species with protection from TB infection and disease.[20] Little PPD-specific cytokine production was observed in BAL CD8+ T cells (Figures S2A–S2E). Local lymphocyte proliferation was observed predominantly after mucosal vaccination (Figure S2F).

Although, by endobronchial instillation, the vaccine was targeted to the lower right lobe, we investigated whether vaccine-induced immune responses would disseminate or be restrained to the targeted lobe only. 3 and 8 weeks after vaccination, we bilaterally collected BAL for immune profiling and found that PPD-specific, cytokine-producing T cells were present in lower right and lower left lung lobes, albeit at a somewhat lower frequency in the non-targeted lobe (Figure 2F). In either lobe, MTBVAC induced earlier and higher responses compared with BCG, including polyfunctional CD4+ Th17 cells.

We also profiled immune responses in lung-draining lymph nodes, the canonical site of T cell priming for respiratory antigenic challenge. PPD-specific IFNγ, TNF-α, and IL-2 production by CD4+ T cells was observed most prominently after mucosal vaccination but was also detectable after intradermal vaccination (Figure S2G). Interestingly, antigen-specific IL17A+ CD4+ T cells were not apparent in these lymph nodes (Figure S2G) because the precursor frequency of these cells was too low to be detected or because Th17 priming occurs elsewhere; for instance, in tertiary lymphoid structures in the lung.[26]

Because we previously also identified IL10 production by unfractionated BAL cells as a correlate of protection, we investigated, by flow cytometry analysis, whether IL-10 production could be T cell derived. Although we confirmed high levels of PPD-specific IL10 production in stimulated BAL cell supernatants after mucosal vaccination with MTBVAC as well as BCG (Figure 2G), by flow cytometry, only very low frequencies of IL-10+ CD4+ T cells were detected in the BAL of mucosally vaccinated animals (Figure 2H). Although the frequencies are low and conclusions therefore little robust , on average, only 2% of IL-17+CD4+ BAL T cells obtained from mucosally vaccinated animals were found to be IL-10+ (data not shown). Thus, it seems that the high levels of IL-10 may not be T cell derived but produced by local innate immune cells in response to innate receptor ligation by mycobacterial compounds in the PPD preparation.

Pulmonary vaccination with MTBVAC induces typically faster and higher polyfunctional CD4+ T cell responses and IL-10 secretion signals associated previously with protection by pulmonary BCG vaccination.

Peripheral immunity after pulmonary vaccination

In parallel to the pulmonary immune responses, we profiled peripheral T cell immunity in search of potential correlates of protection with a perspective for translation to clinical settings. However, as before, when assessing adaptive PPD-specific CD4+ and CD8+ T cell cytokine responses by flow cytometry, no discriminating qualitative signals could be identified that distinguished mucosally from intradermally vaccinated animals. CD4+ T cell cytokine production was observed from week 3 post-vaccination onward and was most prominent in intradermally vaccinated animals and the M.muc group (Figure 3A; Figures S3A–S3D). A slight increase in PPD-specific CD8+ T cell cytokine production was only apparent in the intradermally vaccinated groups 6 weeks post-vaccination (Figure 3B; Figures S4A–S4D). No differences in CD4+ and CD8+ T cell polyfunctionality could be detected.

We used an IFNγ enzyme-linked immune absorbent spot (ELISPOT) assay to assess the breadth of immune responses induced by MTBVAC in comparison with BCG. In line with the flow cytometry data, after stimulation with PPD, which contains antigens shared by BCG and MTBVAC, intradermal MTBVAC was indistinguishable from intradermal BCG by IFNγ secretion (Figure 3C). After stimulation with ESAT6 and CFP10, antigens produced by MTBVAC but absent from BCG, we observed IFNγ production only by peripheral blood mononuclear cells (PBMCs) of MTBVAC-vaccinated animals regardless of vaccination route (Figure 3D). Of note, mucosal MTBVAC appeared to be equally potent in inducing PPD-specific IFNγ signals (Figure 3C). Although we previously observed comparable peripheral immune responses after mucosal and intradermal BCG vaccination, here mucosal BCG vaccination appeared to be less potent in inducing peripheral cytokine production and proliferation (Figures 3A–3C and 3E, respectively).

Figure 2. Pulmonary mucosal vaccination with MTBVAC induces immune signatures associated with protection

Shown is an overview of BAL cell immune responses after mucosal or intradermal vaccination with BCG or MTBVAC.

(A–D) Flow cytometry analysis over time of (A) IFNγ, (B) TNF-α, (C) IL-2, and (D) IL-17A CD4+ T cell responses after vaccination.

(E) Stacked bar graphs depicting CD4+ T cell cytokine polyfunctionality over time after PPD recall stimulation (by group median values).

(F) PPD-specific cytokine production of CD4+ T cells in the lower right and lower left lung lobes at week 3 and week 8, indicating primary and disseminated vaccine responses.

(G) Secretion of IL-10 by unfractionated BAL cells stimulated with PPD at week 8, plotted as culture medium control-corrected values.

(H) Flow cytometry analysis of IL-10 production by CD4+ T cells over time after vaccination.

All graphs show 6 animals per group. In (A)–(D) and (H), + indicates PPD-stimulated samples, and − indicates unstimulated, culture medium-incubated samples as controls. Horizontal lines within bars indicate group medians. Significance of group differences was determined by two-sided Mann-Whitney test adjusted for multiple comparisons. Holms-adjusted $p \leq 0.05$ is depicted. Color coding per individual is consistent throughout the paper.

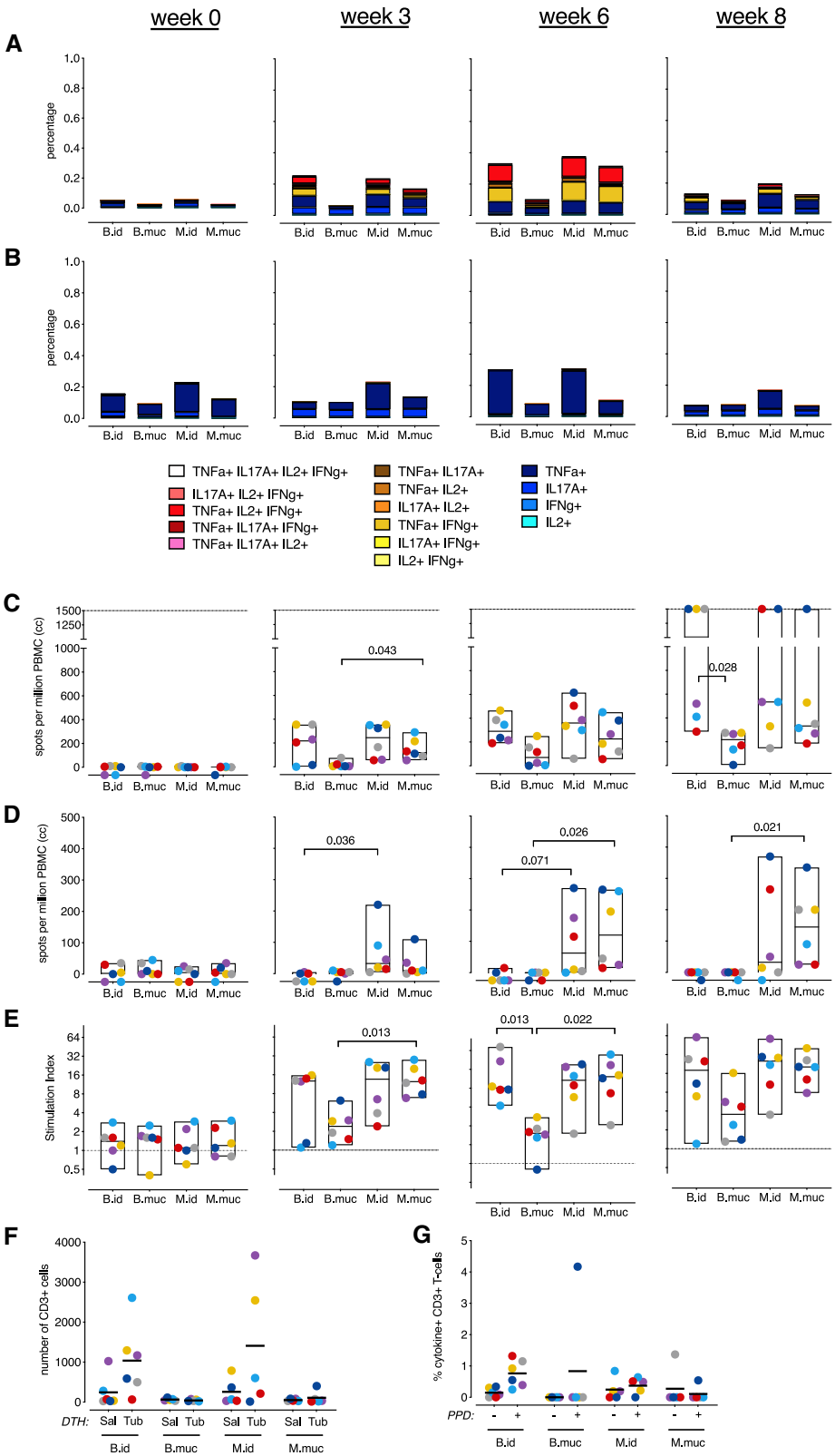

(legend on next page)

As an alternative approach, we investigated the capacity of vaccine-induced T cells by an *in vivo* recall stimulation in TST. To this end, 8 weeks after vaccination, we intradermally injected saline (Sal) or old tuberculin (Tub) on opposite arms of each animal and took biopsies of the injection sites 3 days later. The skin biopsies were subsequently processed and characterized by flow cytometry to measure the delayed type hypersensitivity (DTH) response. By visual inspection of the local skin reaction, redness and swelling appeared after intradermal but not mucosal vaccination (data not shown). Accordingly, a tuberculin-specific influx of antigen-specific CD3+ T cells was exclusively observed in intradermally vaccinated animals (Figure 3F). These T cells showed higher frequencies of cytokine-producing subsets after intradermal vaccination (Figure 3G). When assessing antigen-specific T cells from axillary lymph nodes that drain the TST-DTH skin site, IFNγ-, TNF-α-, and IL-2-producing CD4+ T cells were detectable in intradermally but not mucosally vaccinated animals (Figure S5). So, although mucosal vaccination does result in a peripheral blood response (by flow cytometry and IFNγ ELISPOT), it does not enable these cells to migrate to the site of a skin challenge and, therefore, rules out their analysis for a potential biomarker assay.

The superior induction of local immune responses by mucosal MTBVAC over mucosal BCG was also reflected in the periphery, and these responses appeared to cover a broader range of antigens, including ESAT6/CFP10. However, within the limits of our analyses, no peripheral adaptive responses discriminating between mucosal versus intradermal immunization could be identified.

Mucosal homing marker expression after vaccination

In our search for peripheral correlates of protection, we also considered the possibility that pulmonary rather than intradermal vaccination would imprint peripheral T cells with a higher expression of pulmonary mucosal homing markers. To this end, we assessed the expression of CD103, CXCR3, and CCR5, all known to be involved in homing to the pulmonary mucosa,[27] on peripheral CD4+ T cells by means of flow cytometry.

Prior to vaccination, approximately 25% of circulating CD4+ T cells expressed one or more of these homing markers. After vaccination, either peripherally or mucosally, this percentage did not change, nor was the pattern of homing marker co-expression notably altered in the mucosally vaccinated groups (Figure 4A; Figure S6). Because only a small fraction of all peripheral CD4+ T cells is vaccine specific (Figure 3A), we also assessed homing marker expression of cytokine-producing CD4+ T cells (IFNγ and/or IL-17A). However, because of the low number of cytokine-positive events in the periphery, it was not possible to measure robust and reliable percentages of homing marker expression over time. Using a cutoff of a minimum of 100 cytokine-positive events, we only found robust frequencies 8 weeks post-vaccination. The frequency of homing markers expressed by PPD-specific T cells was comparable with that in the total CD4+ T cell population, although cytokine+ CD4+ T cells from all vaccinated groups consisted of more CCR5 single-positive cells (Figure 4B). When comparing homing marker expression between groups, again, no marked differences between the mucosally and intradermally vaccinated groups were apparent.

Although the aforementioned homing markers did not reveal a peripheral correlate either, we went on to analyze their expression on cytokine-producing T cells in the airways after mucosal vaccination as well as after experimental pulmonary *Mtb* infection. For the latter, samples were obtained from another, independent infection study to characterize protective versus pathogenic BAL responses. Again, we analyzed the expression of CD103, CXCR3, and CCR5 of PPD-specific IFNγ and/or IL-17A-producing T cells. After *Mtb* infection, a high local CD4+ T cell cytokine response is induced, similar to mucosal MTBVAC and higher than mucosal BCG administration (Figure 4C). However, the expression of homing markers was significantly lower in PPD-specific T cells from *Mtb*-infected animals compared with animals vaccinated mucosally with BCG or MTBVAC (Figures 4D and 4E). Although, after *Mtb* infection, approximately 20% of cytokine-producing cells expressed a combination of CD103, CXCR3, and CCR5, 80% of vaccination-induced T cells were positive for one or more of these markers (Figure 4D). In addition to profiling chemokine receptor expression, we also measured CD69 and PD-1 co-expression on cytokine-positive CD4+ T cells as an indicator of a functional tissue-resident phenotype.[28] Previously, we have found that CD69 expression of BAL CD4+ T cells was higher after mucosal over intradermal BCG vaccination and, separately, that IFNγ+TNF-α+IL-2+IL-17A+ T cells expressed higher levels of PD-1.[20] When assessing co-expression of these two markers on IFNγ- and/or IL-17A-producing CD4+ T cells induced by mucosal vaccination, a substantial portion (15%–50%) of these cells was found to co-express both markers. Contrarily, after *Mtb* infection, CD69 and PD1 co-expression on PPD-specific T cells was significantly lower (typically less than 10%) (Figure 4F).

Pulmonary vaccination, associated previously with enhanced protection, results in the presence of antigen-specific T cells

Figure 3. Peripheral immune responses after vaccination

Shown is a characterization of the height and breadth of peripheral immune responses after vaccination.

(A and B) Stacked bar graphs depicting (A) CD4+ and (B) CD8+ T cell cytokine polyfunctionality over time (by group median values) after PPD stimulation.

(C and D) PBMC IFNγ production in response to stimulation with (C) PPD or (D) ESAT6-CFP10 fusion protein, measured by ELISPOT over time.

(E) PPD-specific proliferation of PBMCs, plotted as a stimulation index (the ratio of antigen- over medium control-stimulated values) over time.

(F) T cell numbers in skin biopsies taken (3 days) after intradermal injection of saline (Sal) or old tuberculin (Tub) 8 weeks after vaccination.

(G) PPD-specific cytokine production by T cells from Tub skin biopsies (right panel).

The dotted line in (C) indicates the maximum limit of detection. In (G), + indicates PPD-stimulated samples, and − indicates unstimulated, culture medium-incubated samples as controls. All graphs show 6 animals per group, except for (G), where there are 5 animals for the B.muc, M.id, and M.muc groups. Horizontal lines indicate group medians. Significance of group differences was determined by two-sided Mann-Whitney test adjusted for multiple comparisons. Holms-adjusted $p \leq 0.05$ is depicted. Color coding per individual is consistent throughout.

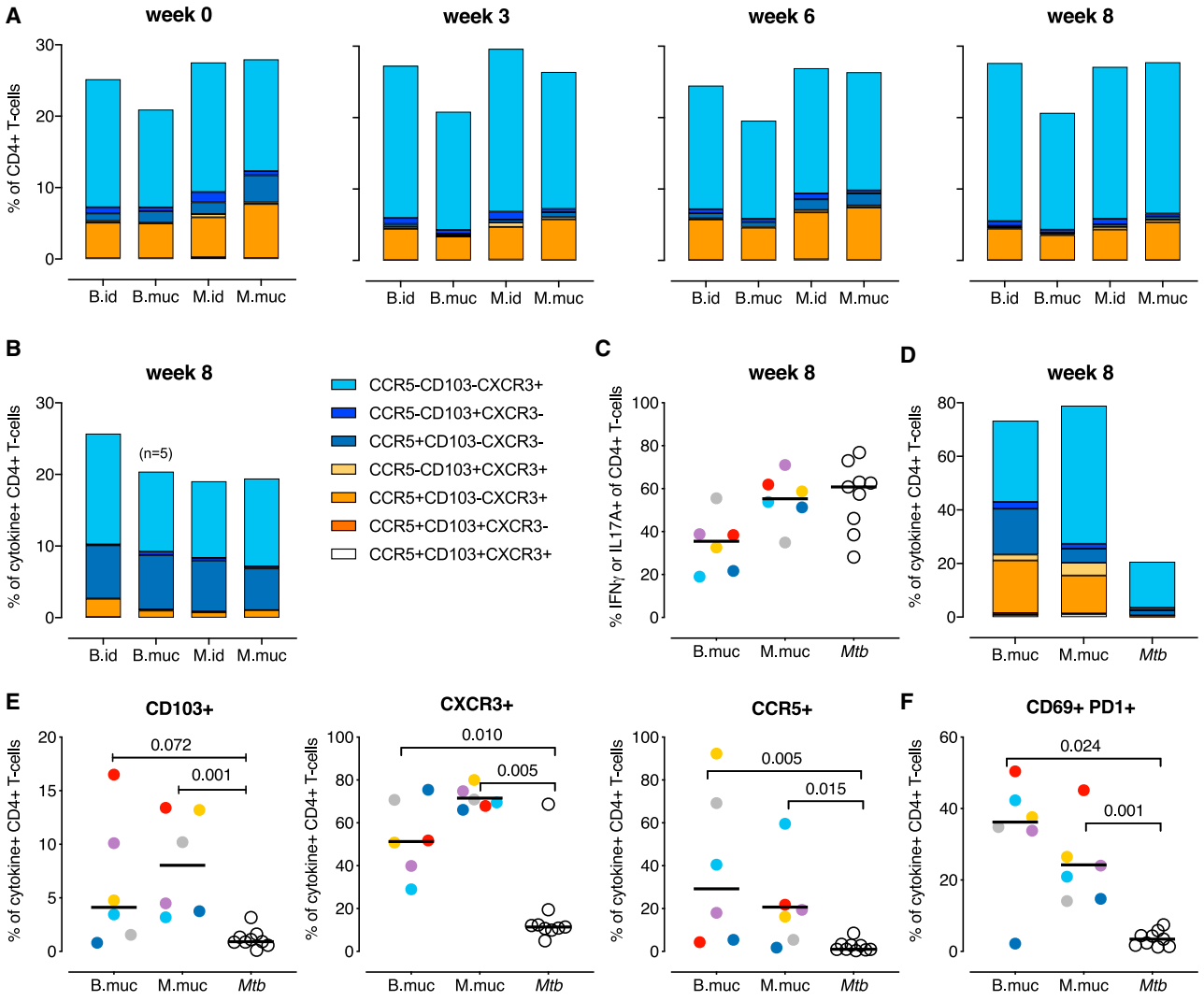

Figure 4. Expression of mucosal homing markers after intradermal and pulmonary vaccination

(A) Expression of CCR5, CD103, and CXCR3 on *ex vivo* CD4+ T cells from peripheral blood over time, depicted as group median values.

(B) CCR5, CD103, and CXCR3 expression by PPD-specific (IFNγ+ and/or IL-17A+) CD4+ T cells from PBMCs at week 8 after vaccination.

(C–E) Comparison of PPD-specific T cells from BALs from pulmonary BCG-vaccinated, MTBVAC-vaccinated, and *Mtb*-infected animals.

(C) Frequencies of IFNγ+ and/or IL-17A+ CD4+ T cells after stimulation with PPD.

(D and E) Expression of CCR5, CD103, and CXCR3 by cytokine+ CD4+ T cells, (D) depicted as group median values (stacked bar graph) or (E) as individual frequencies for separate markers.

(F) Percentage of CD69 and PD1 double-positive cells of cytokine+ CD4+ T cells.

For all graphs, n = 6 animals per group, with the exception of (B) where n = 5 for the BCG.muc group. Horizontal lines indicate group medians. Significance of group differences was determined by two-sided Mann-Whitney test adjusted for multiple comparisons. Holms-adjusted $p \leq 0.05$ is depicted. Color coding per individual is consistent throughout.

with a distinct tissue residency and mucosal homing phenotype. The observation that *Mtb* infection does not elicit this phenotype suggests that these cells could be involved in protection.

Mucosal antibody levels and functionality

In our previously reported vaccination and RLD *Mtb* infection study, mucosal BCG vaccination resulted in pulmonary PPD-specific Ig responses.[20] This observation, in combination with the recent interest in the role of Igs in protection from TB,[29,30] prompted us to investigate the humoral immune response in this study in more detail.

As observed previously for BCG, mucosal vaccination with MTBVAC also resulted in a marked increase in *Mtb*-specific IgA, IgG, and IgM levels in BAL fluid, as detected by ELISA, and in a modest increase in some of the intradermally MTBVAC-vaccinated animals (Figure 5A). Like the cellular immune responses, humoral immunity was found to disseminate from the vaccine-targeted lobe (Figure 5B).

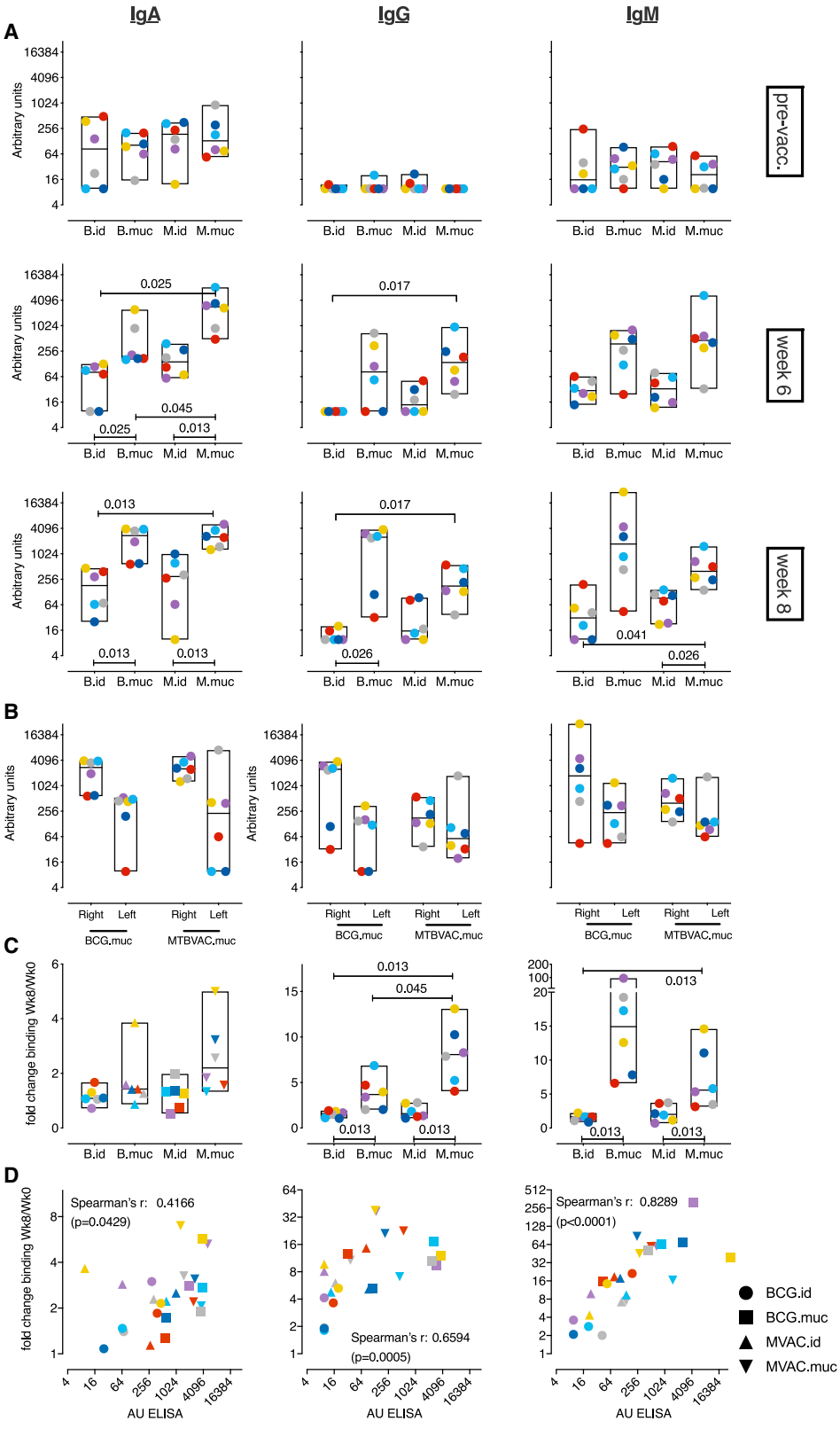

(legend on next page)

To functionally address these humoral immune responses, we assessed the capacity of vaccination-induced Igs to bind to live *Mtb* bacilli. After incubation of dsRed-expressing *Mtb* with BAL fluid, binding of antibodies was measured with biotinylated detection antibodies and phycoerithrin (PE)-conjugated streptavidin on a flow cytometer. After pulmonary but not intradermal vaccination, a distinct increase in PE fluorescence intensity, indicating increased levels of *Mtb*-binding Igs, was observed (Figure 5C). Especially *Mtb*-binding signals for IgG and IgM were elevated significantly in BAL fluid after mucosal vaccination. BAL humoral immune responses, as assessed by ELISA, correlated well with the amount of *Mtb*-bound antibody (Figure 5D).

Last, we investigated whether the antibodies induced by mucosal vaccination would facilitate uptake of *Mtb* by phagocytes. GFP-expressing *Mtb* was incubated with BAL fluid and added to phorbol 12-myristate 13-acetate (PMA)-activated THP-1 cells. After 4 h, the amount of *Mtb*-GFP-positive cells was assessed by flow cytometry. When comparing the amount of *Mtb*+ cells, an increase in uptake of *Mtb* could be observed when the bacteria were incubated with BAL fluid from mucosally but not intradermally vaccinated animals (Figure 6A). To assess the contribution of the different Ig isotypes to this uptake, we correlated the increase in uptake with the increase of *Mtb*-binding Igs induced by vaccination. Of the three isotypes assessed, the amount of vaccination-induced IgG and IgM correlated most strongly with the increase in uptake observed after vaccination (Spearman's rho = 0.6354 with p = 0.0008 and rho = 0.654 with p = 0.0005, respectively; Figure 6B), suggesting that these two isotypes might contribute most to the enhanced uptake of *Mtb* by phagocytes.

DISCUSSION

In this study, pulmonary vaccination with *Mtb*-derived MTBVAC was found to induce pulmonary, PPD-specific, polyfunctional Th17A cells and IL-10 production, an immune signature found previously in association with mucosal BCG-induced protection from TB infection and disease.[20] Compared with *Mtb*-infected animals, PPD-specific T cells in the BAL of animals vaccinated with BCG or MTBVAC through the pulmonary mucosa expressed significantly higher levels of mucosal homing markers. Pulmonary administration of either vaccine also induced Igs in the pulmonary space, of which the IgG and IgM isotypes in particular (more than IgA) were able to bind live *Mtb* and enhance *Mtb* uptake by THP-1 cells. Although equally well tolerated as BCG, MTBVAC induced adaptive responses more rapidly, to a higher magnitude, and, as expected, with broader antigen specificity, whereas such response to *Mtb*-specific ESAT6 and CFP10 has been demonstrated to be key for the improved efficacy of MTBVAC over BCG in mice.[10] Although both mucosal vaccination strategies induced a peripheral immune response in blood, we could not demonstrate an *in vivo* recall response to an antigenic skin challenge, nor could we identify any differential adaptive immune response that could serve as a possible lead for a peripheral correlate of protection. Interestingly, the frequency of innate responders showing trained immunity was increased upon pulmonary vaccination, but these data are beyond the scope of the present manuscript and will be published elsewhere.[31]

Like BCG, we showed that pulmonary delivery of a live attenuated *Mtb* strain also results in the presence of polyfunctional, IL-17A-producing T cells. IL-17A has been associated previously with protection from TB in multiple animal models,[32–34] although the exact mechanisms involved require further elucidation. The effector mechanisms of IL-17A are diverse and can contribute to protection in a number of ways. For example, expression of antimicrobial β-defensin-2 by airway epithelial cells is upregulated after experimental IL-17 treatment,[35] and IL-17A is also known to be involved in neutrophil recruitment to the lungs, which, in turn, has been implied in early protection from TB.[36–38] Additionally, it has been demonstrated that IL-17A is involved in early control of *Mtb* and formation of protective lymphoid follicles.[32,39] However, despite evidence of the protective effect of IL-17A in preclinical models, its precise role in human TB remains to be resolved and is likely dependent on factors such as time, location, and magnitude of IL-17A production as well as conditions of comorbidity and co-infection, including HIV.[40–43]

Compared with *Mtb*-infected animals, PPD-specific BAL T cells from mucosally vaccinated animals were more frequently double-positive for CD69 and PD-1. Although linked to T cell exhaustion in chronic viral infections, PD-1 expression in TB seems to be associated with infection control, as attested by recent reports of TB reactivation after anti-PD-1 treatment.[44,45] In mice, it has been shown that post-*Mtb*-specific PD-1+ CD4+ T cells reside in the lung parenchyma, and adoptive transfer of these, but not of PD1-negative cells, confers superior control of *Mtb* infection.[28] A similar PD-1^{high} lung tissue-resident T cell population has been identified in *Mtb*-infected NHPs.[46] As observed here, the protective PD-1^{high} T cells characterized in the work of Moguche et al.[28] also expressed high levels of CD69 as a marker of activation and tissue residency in the lungs and lymph nodes.[47–49] Of note, a recent NHP *Mtb* study reported superior protection and increased frequencies of CD69+ T cells in the lung parenchyma after intravenous BCG vaccination compared with aerosol BCG administration.[24]. Interestingly, in the latter study, endobronchial

Figure 5. Vaccine-induced humoral immune responses at the pulmonary mucosa

(A) Magnitude of *Mtb* whole-cell lysate (WCL)-specific immunoglobulin (Ig) type A, G, and M responses in BAL over time.

(B) *Mtb* WCL-specific Ig levels in the lower right (vaccinated) and lower left (unvaccinated) lung lobe at week 8.

Antibody levels in (A) and (B) are plotted as arbitrary units, as determined by standardization against a reference sample.

(C) Binding of BAL Igs to live *Mtb*, depicted as the fold change in geometric mean fluorescence intensity (GMFI) of Ig-specific detection antibody signals between week 0 and week 8 post-vaccination.

(D) Correlation between *Mtb* WCL-specific Ig levels (in arbitrary units) and Ig binding to live *Mtb* (as fold change compared with control) 8 weeks after vaccination.

For all graphs, n = 6 animals per group. Horizontal lines indicate group medians. Color coding per individual is consistent throughout. Significance of group differences was determined by two-sided Mann-Whitney test adjusted for multiple comparisons. Holms-adjusted $p \leq 0.05$ is depicted. Correlations in (D) were calculated with Spearman's rank order test.

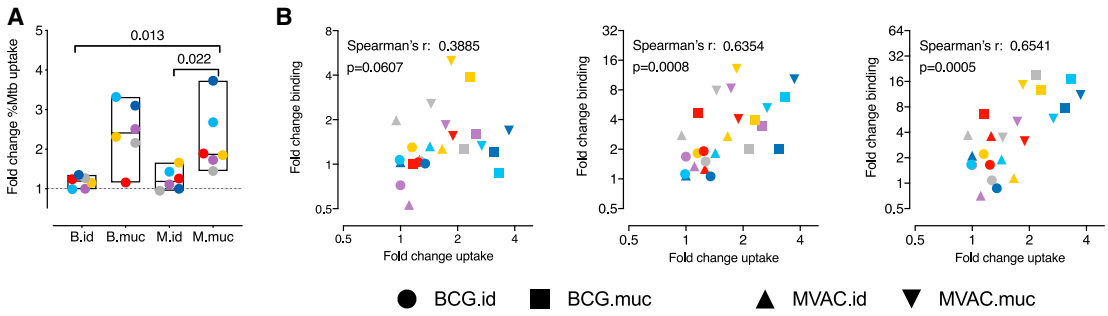

Figure 6. Vaccine-mediated uptake of *Mtb* by phagocytes

(A) Uptake of *Mtb* by PMA-activated THP1 cells after incubation with BAL fluid obtained before and 8 weeks after vaccination, depicted as the fold change in the percentage of *Mtb*+ THP1 cells.

(B) Correlation between vaccination-induced Igs capable of binding to live *Mtb*, from left to right for IgA, IgG, and IgM, and the change in *Mtb* uptake.

For all graphs, n = 6 animals per group. Horizontal lines indicate group medians. Color coding per individual is consistent throughout. Significance of group differences was determined by two-sided Mann-Whitney test adjusted for multiple comparisons. Holms-adjusted $p \leq 0.05$ is depicted. Correlations in (B) were calculated with Spearman's rank order test.

BCG vaccination also induced increased frequencies of these cells in the lungs, although these animals were not challenged with *Mtb*.

In addition to CD69 and PD1, PPD-specific T cells induced by mucosal vaccination also more frequently expressed CD103, CXCR3, and CCR5, which are associated with mucosal homing and tissue residency. Mucosal vaccination with *Bacillus subtilis* spores expressing *Mtb* antigens boosted protection conferred by BCG and associated with induction of CD103+CD69+ tissue-resident T cells in mice.[50] CXCR3 has been identified as crucial for T cell entry into the lung parenchyma.[51] In *Mtb*-infected NHPs, CD4+ T cells expressing CXCR3 and CCR5 were identified in granulomatous tissue, but these cells did not colocalize with *Mtb*-infected macrophages in the granuloma center and, therefore, seem unable to exert their effector function.[46,52] Nevertheless, vaccine-induced presence of high frequencies of these cells during the early stages of infection and granuloma formation might contribute to control of *Mtb* by (alveolar) macrophages.

Mucosal MTBVAC and BCG vaccination resulted in the presence of *Mtb*-specific Igs at the site of infection. Especially IgG and IgM in BAL were able to bind live *Mtb* and enhanced phagocytosis, whereas IgA showed the least amount of binding and only a weak correlation between Ig binding to *Mtb* and phagocyte uptake. Although enhanced Ig was not a formal statistical correlate of protection in our previous study, evidence of the protective potential of *Mtb*-specific antibodies has been reported recently in various papers. Boosting BCG-primed mice with heat-killed MTBVAC via the respiratory mucosa enhanced protection, which was dependent on expression of the polymeric Ig receptor and, thus, suggestive of the protective role of Ig.[53] Of note, in that same paper, NHPs boosted with heat-killed MTBVAC via the respiratory route showed local induction of antibodies that, as observed here, were functional in binding and phagocytosis of *Mtb*. Moreover, *Mtb*-specific IgA clones isolated from individuals with TB have been shown to be able to restrict *Mtb* replication in a lung epithelial cell line.[54] Also, elevated IgG titers to BCG have been found in association with protection against *Mtb* infection,[55] and serum IgG from BCG-vaccinated individuals was able to inhibit intracellular growth of mycobacteria.[56] Interestingly, highly exposed individuals that remained IGRA-negative, so-called resisters, exhibited enhanced antibody responses to *Mtb*.[57] *Mtb*-specific antibodies could contribute to protection in various ways, including enhancement of *Mtb* phagocytosis as observed here, activation of the inflammasome, and/or facilitation of antibody-dependent cell-mediated cytotoxicity (ADCC).[29,58]

The protective efficacy of MTBVAC has been linked to immune reactivity to *Mtb*-specific ESAT-6 and CFP-10 antigens,[10] whose induction was also observed in our study. However, the current standard in diagnosing latent TB infection is detection of discriminatory IFNγ responses by stimulation of peripheral blood with *Mtb*-specific antigens, including ESAT-6. Indeed, MTBVAC-vaccinated neonates showed dose-dependent conversion in an IFNγ release assay (IGRA) 180 days post-vaccination, which would interfere with diagnosis of TB.[12] Further exploration of the dynamics of IGRA conversion after MTBVAC vaccination is required to assess the usefulness of the IGRA as a TB diagnostic after MTBVAC administration. Ideally, for successful deployment of MTBVAC as a vaccine, regardless of the route of administration, new diagnostic tools not dependent on T cell epitopes shared by *Mtb* and MTBVAC need to be developed.

In this study (as well as in our previous work[20]), pulmonary vaccination was established through endobronchial vaccine instillation. Although here we show that targeting a particular lung lobe by endobronchial instillation results in contralateral dissemination of the ensuing vaccine-induced immune response (cellular and humoral), it remains to be formally established whether this would also result in protection against contralateral challenge. From a translational perspective, however, we must conclude that endobronchial instillation is incompatible with clinical vaccination. For other, more translatable mucosal delivery strategies, such as aerosol, intranasal, or oral administration, the issue of contralateral protection appears to be less relevant. Such alternative delivery strategies, however, must be explored in more detail to assess whether BCG or MTBVAC would induce improved protection. Although in mice and guinea

pigs aerosol/intranasal BCG vaccination showed increased efficacy compared with parenteral administration,[59,60] data on the protective efficacy of aerosol vaccination of NHPs is contradictory and so far inconclusive. Early work with macaques has shown increased protection by aerosol-delivered BCG compared with intradermal BCG, on par with intravenous BCG vaccination.[17] Contrarily, in a recent macaque study, aerosol BCG vaccination did not confer superior protection.[24] This discrepancy in protective efficacy could be caused by a variety of factors, including dose, efficiency, and viability of the vaccine delivered. Studies directly comparing mucosal vaccination routes are required to identify which conditions are essential for inducing protection. In humans, aerosol vaccination with BCG has been explored in the 1960s and found to induce dose-dependent TST conversion.[61] New studies of BCG administration by aerosol have been initiated recently (NCT03912207). A study exploring endobronchial BCG instillation with the aim of developing a controlled human infection model also reported no serious adverse events.[62] From historic data, it can be inferred that, in humans, oral BCG administration is at least as effective as intradermal injection. Oral administration was the initial route of vaccination when BCG was deployed as a pediatric vaccine in the 1920s, and in Brazil, BCG was routinely administered orally until the 1970s.[63] Recent studies investigating oral BCG vaccination report no safety concerns, and, as observed here, oral administration induced *Mtb*-specific mucosal IgA and CXCR3-expressing T cells in BAL.[64,65]

Our data argue for further investigation of pulmonary mucosal administration of MTBVAC and its protective capacity in particular because it potentially comprises a more efficacious vaccination strategy than intradermal BCG to combat TB.

Limitations of study

The present paper builds on our previous work that has shown that pulmonary mucosal delivery of *M. bovis* BCG confers improved protection from TB infection and disease in a repeated limiting dose *M. tuberculosis* challenge model in rhesus macaques. Despite the fact that MTBVAC provides broader antigenic specificity and, upon mucosal delivery, has been found to be as potent as BCG in inducing a local immune signature also associated with enhanced protection, this study, by design, does not directly address the protective efficacy of (pulmonary mucosal) MTBVAC. To this end, a follow-up study will be required that shall include infectious challenge after vaccination.

Moreover, none of the present efforts identify a readily translatable lead for a peripheral immune correlate as a surrogate for the local immune signature conferred by pulmonary mucosal delivery with BCG or MTBVAC. Neither characterization of the peripheral immune response in blood nor the DTH response after TST positively discriminate the more efficacious mucosal route from standard intradermal vaccine administration. The lack of such a correlate from a readily accessible site or tissue hinders development of a biomarker assay that would critically enhance clinical evaluation of new TB vaccine candidates or vaccination strategies.

Although prior immune correlates in the alveolar space are corroborated and extended by identification of increased local homing and tissue residency markers on antigen-specific T cells and phagocytosis-enhancing antibodies, this study sheds no light on mechanisms that underly development of tissue-resident T cell subsets or the protective mechanisms of IL-17, IL-10, or antigen-specific antibodies. Although associated circumstantially, their exact roles in mucosal immune surveillance, regulation, and prevention of infection-associated lung pathology and/or mycobactericidal activity remain to be investigated further.

In the context of translation, pulmonary vaccination by bronchoscope, as deployed in this study, is suitable for proof of concept but not amenable for (larger-scale) clinical vaccination campaigns. Alternative administration of TB vaccines via respiratory or other mucosal surfaces requires more explorative research, in particular also for (aerosolized delivery of) live attenuated whole-cell vaccines.

STAR★METHODS

Detailed methods are provided in the online version of this paper and include the following:

- KEY RESOURCES TABLE
- RESOURCE AVAILABILITY
  - Lead contact
  - Materials availability
  - Data and code availability
- EXPERIMENTAL MODEL AND SUBJECT DETAILS
  - Ethics & Animal Handling
  - Vaccines, Vaccine Preparation & Administration
  - Mtb Infection
  - Biosample Collection & Processing
- METHOD DETAILS
  - Flow cytometry
  - Luminex
  - IFNγ ELISPOT
  - Immunoglobulin ELISA
  - Mtb binding and phagocytosis assay
- QUANTIFICATION AND STATISTICAL ANALYSIS

SUPPLEMENTAL INFORMATION

Supplemental Information can be found online at https://doi.org/10.1016/j.xcrm.2020.100187.

ACKNOWLEDGMENTS

We thank BPRC's animal and veterinary care teams as well as the pathology team and clinical lab personnel for their outstanding contributions to this work. We thank Dr. E. Remarque for advice regarding statistical analysis and F. van Hassel for support with graphics. We thank Prof. T. Ottenhoff at Leiden University Medical Centre for providing *Mtb*-dsRed and Kees Franken and his lab for the ESAT6-CFP10 fusion protein. The following reagent was obtained through BEI Resources, NIAID, NIH: *Mycobacterium tuberculosis*, Strain Erdman Barcode Library, NR-50781. This NHP study and the MTBVAC vaccine are linked to the TB vaccine R&D program of the TuBerculosis Vaccine Initiative(TBVI)-governed TBVAC2020 Consortium, supported by the European Commission under the Horizon 2020 program, grant agreement 643381. Extended immune response analyses were in part supported as a research effort of the TRANSVAC2 Consortium, also under the Horizon 2020 program, grant agreement 730964.

AUTHOR CONTRIBUTIONS

Conceptualization and Supervision, K.D., C.H.M.K., and F.A.W.V.; Study Design and Methodology Detailing, K.D., F.A.W.V., M.P.M.V., N.A., D.M., C.M., J.T., E.R., and E.P.; Assay Performance, Data Processing, and Analysis, K.D., N.A., C.B., S.O.H., C.C.S., R.A.W.V., K.G.H., and M.P.M.V.; First Version Paper Drafting, K.D. and F.A.W.V.

DECLARATION OF INTERESTS

E.R., E.P., N.A., and C.M. are co-inventors on a patent-entitled tuberculosis vaccine held by the University of Zaragoza and Biofabri. E.R. and E.P. are employees of Biofabri. J.T. is an employee of TuBerculosis Vaccine Initiative and advisor to Biofabri.

Received: May 20, 2020
Revised: October 23, 2020
Accepted: December 17, 2020
Published: January 19, 2021

REFERENCES

1. WHO (2019). World Health Organization. Global tuberculosis report 2019 (WHO).
2. Mangtani, P., Abubakar, I., Ariti, C., Beynon, R., Pimpin, L., Fine, P.E., Rodrigues, L.C., Smith, P.G., Lipman, M., Whiting, P.F., et al. (2014). Protection by BCG vaccine against tuberculosis: a systematic review of randomized controlled trials. Clin. Infect. Dis. *58*, 470–480.
3. Brandt, L., Feino Cunha, J., Weinreich Olsen, A., Chilima, B., Hirsch, P., Appelberg, R., and Andersen, P. (2002). Failure of the Mycobacterium bovis BCG vaccine: some species of environmental mycobacteria block multiplication of BCG and induction of protective immunity to tuberculosis. Infect. Immun. *70*, 672–678.
4. Zhang, L., Ru, H.W., Chen, F.Z., Jin, C.Y., Sun, R.F., Fan, X.Y., Guo, M., Mai, J.T., Xu, W.X., Lin, Q.X., and Liu, J. (2016). Variable Virulence and Efficacy of BCG Vaccine Strains in Mice and Correlation With Genome Polymorphisms. Mol. Ther. *24*, 398–405.
5. Sable, S.B., Posey, J.E., and Scriba, T.J. (2019). Tuberculosis Vaccine Development: Progress in Clinical Evaluation. Clin. Microbiol. Rev. *33*, e00100-19.
6. Voss, G., Casimiro, D., Neyrolles, O., Williams, A., Kaufmann, S.H.E., McShane, H., Hatherill, M., and Fletcher, H.A. (2018). Progress and challenges in TB vaccine development. F1000Res. *7*, 199.
7. Arbues, A., Aguilo, J.I., Gonzalo-Asensio, J., Marinova, D., Uranga, S., Puentes, E., Fernandez, C., Parra, A., Cardona, P.J., Vilaplana, C., et al. (2013). Construction, characterization and preclinical evaluation of MTBVAC, the first live-attenuated M. tuberculosis-based vaccine to enter clinical trials. Vaccine *31*, 4867–4873.
8. Pérez, I., Uranga, S., Sayes, F., Frigui, W., Samper, S., Arbués, A., Aguiló, N., Brosch, R., Martín, C., and Gonzalo-Asensio, J. (2020). Live attenuated TB vaccines representing the three modern Mycobacterium tuberculosis lineages reveal that the Euro-American genetic background confers optimal vaccine potential. EBioMedicine *55*, 102761.
9. Gonzalo-Asensio, J., Marinova, D., Martin, C., and Aguilo, N. (2017). MTBVAC: Attenuating the Human Pathogen of Tuberculosis (TB) Toward a Promising Vaccine against the TB Epidemic. Front. Immunol. *8*, 1803.
10. Aguilo, N., Gonzalo-Asensio, J., Alvarez-Arguedas, S., Marinova, D., Gomez, A.B., Uranga, S., Spallek, R., Singh, M., Audran, R., Spertini, F., and Martin, C. (2017). Reactogenicity to major tuberculosis antigens absent in BCG is linked to improved protection against Mycobacterium tuberculosis. Nat. Commun. *8*, 16085.
11. Spertini, F., Audran, R., Chakour, R., Karoui, O., Steiner-Monard, V., Thierry, A.-C., Mayor, C.E., Rettby, N., Jaton, K., Vallotton, L., et al. (2015). Safety of human immunisation with a live-attenuated Mycobacterium tuberculosis vaccine: a randomised, double-blind, controlled phase I trial. Lancet Respir. Med. *3*, 953–962.
12. Tameris, M., Mearns, H., Penn-Nicholson, A., Gregg, Y., Bilek, N., Mabwe, S., Geldenhuys, H., Shenje, J., Luabeya, A.K.K., Murillo, I., et al.; MTBVAC Clinical Trial Team (2019). Live-attenuated Mycobacterium tuberculosis vaccine MTBVAC versus BCG in adults and neonates: a randomised controlled, double-blind dose-escalation trial. Lancet Respir. Med. *7*, 757–770.
13. Aguilo, N., Uranga, S., Marinova, D., Monzon, M., Badiola, J., and Martin, C. (2016). MTBVAC vaccine is safe, immunogenic and confers protective efficacy against Mycobacterium tuberculosis in newborn mice. Tuberculosis (Edinb.) *96*, 71–74.
14. Clark, S., Lanni, F., Marinova, D., Rayner, E., Martin, C., and Williams, A. (2017). Revaccination of Guinea Pigs With the Live Attenuated Mycobacterium tuberculosis Vaccine MTBVAC Improves BCG's Protection Against Tuberculosis. J. Infect. Dis. *216*, 525–533.
15. White, A., Sibley, L., Sarfas, C., Morrison, A., Gullick, J., Gleeson, F., McIntyre, A., Simon, C., Lindestam, C., Sette, A., et al. (2020). MTBVAC vaccination protects rhesus macaques against aerosol challenge with M. tuberculosis and induces immune signatures analogous to those observed in clinical studies. NPJ Vaccines. https://doi.org/10.1038/s41541-020-00262-8.
16. Aguilo, N., Alvarez-Arguedas, S., Uranga, S., Marinova, D., Monzon, M., Badiola, J., and Martin, C. (2016). Pulmonary but Not Subcutaneous Delivery of BCG Vaccine Confers Protection to Tuberculosis-Susceptible Mice by an Interleukin 17-Dependent Mechanism. J. Infect. Dis. *213*, 831–839.
17. Barclay, W.R., Busey, W.M., Dalgard, D.W., Good, R.C., Janicki, B.W., Kasik, J.E., Ribi, E., Ulrich, C.E., and Wolinsky, E. (1973). Protection of monkeys against airborne tuberculosis by aerosol vaccination with bacillus Calmette-Guerin. Am. Rev. Respir. Dis. *107*, 351–358.
18. Perdomo, C., Zedler, U., Kühl, A.A., Lozza, L., Saikali, P., Sander, L.E., Vogelzang, A., Kaufmann, S.H., and Kupz, A. (2016). Mucosal BCG Vaccination Induces Protective Lung-Resident Memory T Cell Populations against Tuberculosis. mBio *7*, e01686-16.
19. Verreck, F.A.W., Tchilian, E.Z., Vervenne, R.A.W., Sombroek, C.C., Kondova, I., Eissen, O.A., Sommandas, V., van der Werff, N.M., Verschoor, E., Braskamp, G., et al. (2017). Variable BCG efficacy in rhesus populations: Pulmonary BCG provides protection where standard intra-dermal vaccination fails. Tuberculosis (Edinb.) *104*, 46–57.
20. Dijkman, K., Sombroek, C.C., Vervenne, R.A.W., Hofman, S.O., Boot, C., Remarque, E.J., Kocken, C.H.M., Ottenhoff, T.H.M., Kondova, I., Khayum, M.A., et al. (2019). Prevention of tuberculosis infection and disease by local BCG in repeatedly exposed rhesus macaques. Nat. Med. *25*, 255–262.
21. Cardona, P.J., and Williams, A. (2017). Experimental animal modelling for TB vaccine development. Int. J. Infect. Dis. *56*, 268–273.
22. Hunter, R.L., Actor, J.K., Hwang, S.A., Khan, A., Urbanowski, M.E., Kaushal, D., and Jagannath, C. (2018). Pathogenesis and Animal Models of Post-Primary (Bronchogenic) Tuberculosis, A Review. Pathogens *7*, 19.
23. Moliva, J.I., Hossfeld, A.P., Canan, C.H., Dwivedi, V., Wewers, M.D., Beamer, G., Turner, J., and Torrelles, J.B. (2018). Exposure to human alveolar lining fluid enhances Mycobacterium bovis BCG vaccine efficacy against Mycobacterium tuberculosis infection in a CD8(+) T-cell-dependent manner. Mucosal Immunol. *11*, 968–978.
24. Darrah, P.A., Zeppa, J.J., Maiello, P., Hackney, J.A., Wadsworth, M.H., 2nd, Hughes, T.K., Pokkali, S., Swanson, P.A., 2nd, Grant, N.L., Rodgers, M.A., et al. (2020). Prevention of tuberculosis in macaques after intravenous BCG immunization. Nature *577*, 95–102.
25. Sharpe, S., White, A., Sarfas, C., Sibley, L., Gleeson, F., McIntyre, A., Basaraba, R., Clark, S., Hall, G., Rayner, E., et al. (2016). Alternative BCG delivery strategies improve protection against Mycobacterium tuberculosis in non-human primates: Protection associated with mycobacterial antigen-specific CD4 effector memory T-cell populations. Tuberculosis (Edinb.) *101*, 174–190.

26. Kaushal, D., Foreman, T.W., Gautam, U.S., Alvarez, X., Adekambi, T., Rangel-Moreno, J., Golden, N.A., Johnson, A.M., Phillips, B.L., Ahsan, M.H., et al. (2015). Mucosal vaccination with attenuated Mycobacterium tuberculosis induces strong central memory responses and protects against tuberculosis. Nat. Commun. *6*, 8533.

27. Iijima, N., and Iwasaki, A. (2015). Tissue instruction for migration and retention of TRM cells. Trends Immunol. *36*, 556–564.

28. Moguche, A.O., Shafiani, S., Clemons, C., Larson, R.P., Dinh, C., Higdon, L.E., Cambier, C.J., Sissons, J.R., Gallegos, A.M., Fink, P.J., and Urdahl, K.B. (2015). ICOS and Bcl6-dependent pathways maintain a CD4 T cell population with memory-like properties during tuberculosis. J. Exp. Med. *212*, 715–728.

29. Kawahara, J.Y., Irvine, E.B., and Alter, G. (2019). A Case for Antibodies as Mechanistic Correlates of Immunity in Tuberculosis. Front. Immunol. *10*, 996.

30. Tran, A.C., Kim, M.Y., and Reljic, R. (2019). Emerging Themes for the Role of Antibodies in Tuberculosis. Immune Netw. *19*, e24.

31. Vierboom, M.P.M., Dijkman, K., Sombroek, C.C., Hofman, S.O., Boot, C., Vervenne, R.A.W., Haanstra, K.G., van der Sande, M., van Emst, L., Domínguez-Andrés, J., et al. (2021). Stronger induction of trained immunity by mucosal BCG or MTBVAC vaccination compared to standard intradermal vaccination. Cell Rep. Med. *2*, this issue.

32. Gopal, R., Monin, L., Slight, S., Uche, U., Blanchard, E., Fallert Junecko, B.A., Ramos-Payan, R., Stallings, C.L., Reinhart, T.A., Kolls, J.K., et al. (2014). Unexpected role for IL-17 in protective immunity against hypervirulent Mycobacterium tuberculosis HN878 infection. PLoS Pathog. *10*, e1004099.

33. Wareham, A.S., Tree, J.A., Marsh, P.D., Butcher, P.D., Dennis, M., and Sharpe, S.A. (2014). Evidence for a role for interleukin-17, Th17 cells and iron homeostasis in protective immunity against tuberculosis in cynomolgus macaques. PLoS ONE *9*, e88149.

34. Wozniak, T.M., Saunders, B.M., Ryan, A.A., and Britton, W.J. (2010). Mycobacterium bovis BCG-specific Th17 cells confer partial protection against Mycobacterium tuberculosis infection in the absence of gamma interferon. Infect. Immun. *78*, 4187–4194.

35. Kao, C.Y., Chen, Y., Thai, P., Wachi, S., Huang, F., Kim, C., Harper, R.W., and Wu, R. (2004). IL-17 markedly up-regulates beta-defensin-2 expression in human airway epithelium via JAK and NF-kappaB signaling pathways. J. Immunol. *173*, 3482–3491.

36. Hilda, J.N., Das, S., Tripathy, S.P., and Hanna, L.E. (2020). Role of neutrophils in tuberculosis: A bird's eye view. Innate Immun. *26*, 240–247.

37. Miyamoto, M., Prause, O., Sjostrand, M., Laan, M., Lotvall, J., and Linden, A. (2003). Endogenous IL-17 as a mediator of neutrophil recruitment caused by endotoxin exposure in mouse airways. J. Immunol. *170*, 4665–4672.

38. Shenoy, A.T., Wasserman, G.A., Arafa, E.I., Wooten, A.K., Smith, N.M.S., Martin, I.M.C., Jones, M.R., Quinton, L.J., and Mizgerd, J.P. (2020). Lung CD4(+) resident memory T cells remodel epithelial responses to accelerate neutrophil recruitment during pneumonia. Mucosal Immunol. *13*, 334–343.

39. Ardain, A., Domingo-Gonzalez, R., Das, S., Kazer, S.W., Howard, N.C., Singh, A., Ahmed, M., Nhamoyebonde, S., Rangel-Moreno, J., Ogongo, P., et al. (2019). Group 3 innate lymphoid cells mediate early protective immunity against tuberculosis. Nature *570*, 528–532.

40. Devalraju, K.P., Neela, V.S.K., Ramaseri, S.S., Chaudhury, A., Van, A., Krovvidi, S.S., Vankayalapati, R., and Valluri, V.L. (2018). IL-17 and IL-22 production in HIV+ individuals with latent and active tuberculosis. BMC Infect. Dis. *18*, 321.

41. Elhed, A., and Unutmaz, D. (2010). Th17 cells and HIV infection. Curr. Opin. HIV AIDS *5*, 146–150.

42. Shen, H., and Chen, Z.W. (2018). The crucial roles of Th17-related cytokines/signal pathways in M. tuberculosis infection. Cell. Mol. Immunol. *15*, 216–225.

43. Torrado, E., and Cooper, A.M. (2010). IL-17 and Th17 cells in tuberculosis. Cytokine Growth Factor Rev. *21*, 455–462.

44. Jensen, K.H., Persson, G., Bondgaard, A.L., and Pøhl, M. (2018). Development of pulmonary tuberculosis following treatment with anti-PD-1 for non-small cell lung cancer. Acta Oncol. *57*, 1127–1128.

45. Picchi, H., Mateus, C., Chouaid, C., Besse, B., Marabelle, A., Michot, J.M., Champiat, S., Voisin, A.L., and Lambotte, O. (2018). Infectious complications associated with the use of immune checkpoint inhibitors in oncology: Reactivation of tuberculosis after anti PD-1 treatment. Clin. Microbiol. Infect. *24*, 216–218.

46. Kauffman, K.D., Sallin, M.A., Sakai, S., Kamenyeva, O., Kabat, J., Weiner, D., Sutphin, M., Schimel, D., Via, L., Barry, C.E., 3rd., et al. (2018). Defective positioning in granulomas but not lung-homing limits CD4 T-cell interactions with Mycobacterium tuberculosis-infected macrophages in rhesus macaques. Mucosal Immunol. *11*, 462–473.

47. Kumar, B.V., Ma, W., Miron, M., Granot, T., Guyer, R.S., Carpenter, D.J., Senda, T., Sun, X., Ho, S.H., Lerner, H., et al. (2017). Human Tissue-Resident Memory T Cells Are Defined by Core Transcriptional and Functional Signatures in Lymphoid and Mucosal Sites. Cell Rep. *20*, 2921–2934.

48. Purwar, R., Campbell, J., Murphy, G., Richards, W.G., Clark, R.A., and Kupper, T.S. (2011). Resident memory T cells (T(RM)) are abundant in human lung: diversity, function, and antigen specificity. PLoS ONE *6*, e16245.

49. Shiow, L.R., Rosen, D.B., Brdicková, N., Xu, Y., An, J., Lanier, L.L., Cyster, J.G., and Matloubian, M. (2006). CD69 acts downstream of interferon-alpha/beta to inhibit S1P1 and lymphocyte egress from lymphoid organs. Nature *440*, 540–544.

50. Copland, A., Diogo, G.R., Hart, P., Harris, S., Tran, A.C., Paul, M.J., Singh, M., Cutting, S.M., and Reljic, R. (2018). Mucosal Delivery of Fusion Proteins with *Bacillus subtilis* Spores Enhances Protection against Tuberculosis by Bacillus Calmette-Guérin. Front. Immunol. *9*, 346.

51. Jeyanathan, M., Afkhami, S., Khera, A., Mandur, T., Damjanovic, D., Yao, Y., Lai, R., Haddadi, S., Dvorkin-Gheva, A., Jordana, M., et al. (2017). CXCR3 Signaling Is Required for Restricted Homing of Parenteral Tuberculosis Vaccine-Induced T Cells to Both the Lung Parenchyma and Airway. J. Immunol. *199*, 2555–2569.

52. Lin, P.L., Pawar, S., Myers, A., Pegu, A., Fuhrman, C., Reinhart, T.A., Capuano, S.V., Klein, E., and Flynn, J.L. (2006). Early events in Mycobacterium tuberculosis infection in cynomolgus macaques. Infect. Immun. *74*, 3790–3803.

53. Aguilo, N., Uranga, S., Mata, E., Tarancon, R., Gómez, A.B., Marinova, D., Otal, I., Monzón, M., Badiola, J., Montenegro, D., et al. (2020). Respiratory Immunization With a Whole Cell Inactivated Vaccine Induces Functional Mucosal Immunoglobulins Against Tuberculosis in Mice and Non-human Primates. Front. Microbiol. *11*, 1339.

54. Zimmermann, N., Thormann, V., Hu, B., Köhler, A.B., Imai-Matsushima, A., Locht, C., Arnett, E., Schlesinger, L.S., Zoller, T., Schürmann, M., et al. (2016). Human isotype-dependent inhibitory antibody responses against Mycobacterium tuberculosis. EMBO Mol. Med. *8*, 1325–1339.

55. Logan, E., Luabeya, A.K.K., Mulenga, H., Mrdjen, D., Ontong, C., Cunningham, A.F., Tameris, M., McShane, H., Scriba, T.J., Horsnell, W.G.C., and Hatherill, M. (2018). Elevated IgG Responses in Infants Are Associated With Reduced Prevalence of *Mycobacterium tuberculosis* Infection. Front. Immunol. *9*, 1529.

56. Chen, T., Blanc, C., Eder, A.Z., Prados-Rosales, R., Souza, A.C., Kim, R.S., Glatman-Freedman, A., Joe, M., Bai, Y., Lowary, T.L., et al. (2016). Association of Human Antibodies to Arabinomannan With Enhanced Mycobacterial Opsonophagocytosis and Intracellular Growth Reduction. J. Infect. Dis. *214*, 300–310.

57. Lu, L.L., Smith, M.T., Yu, K.K.Q., Luedemann, C., Suscovich, T.J., Grace, P.S., Cain, A., Yu, W.H., McKitrick, T.R., Lauffenburger, D., et al. (2019). IFN-γ-independent immune markers of Mycobacterium tuberculosis exposure. Nat. Med. *25*, 977–987.

58. Li, H., and Javid, B. (2018). Antibodies and tuberculosis: finally coming of age? Nat. Rev. Immunol. *18*, 591–596.

59. Chen, L., Wang, J., Zganiacz, A., and Xing, Z. (2004). Single intranasal mucosal Mycobacterium bovis BCG vaccination confers improved protection compared to subcutaneous vaccination against pulmonary tuberculosis. Infect. Immun. *72*, 238–246.

60. Garcia-Contreras, L., Wong, Y.L., Muttil, P., Padilla, D., Sadoff, J., Derousse, J., Germishuizen, W.A., Goonesekera, S., Elbert, K., Bloom, B.R., et al. (2008). Immunization by a bacterial aerosol. Proc. Natl. Acad. Sci. USA *105*, 4656–4660.

61. Rosenthal, S.R., McEnery, J.T., and Raisys, N. (1968). Aerogenic BCG vaccination against tuberculosis in animal and human subjects. J. Asthma Res. *5*, 309–323.

62. Davids, M., Pooran, A., Hermann, C., Mottay, L., Thompson, F., Cardenas, J., Gu, J., Koeuth, T., Meldau, R., Limberis, J., et al. (2019). A Human Lung Challenge Model to Evaluate the Safety and Immunogenicity of PPD and Live BCG. Am. J. Respir. Crit. Care Med. *201*, 1277–1291.

63. Benévolo-de-Andrade, T.C., Monteiro-Maia, R., Cosgrove, C., and Castello-Branco, L.R.R. (2005). BCG Moreau Rio de Janeiro: an oral vaccine against tuberculosis–review. Mem. Inst. Oswaldo Cruz *100*, 459–465.

64. Cosgrove, C.A., Castello-Branco, L.R., Hussell, T., Sexton, A., Giemza, R., Phillips, R., Williams, A., Griffin, G.E., Dougan, G., and Lewis, D.J. (2006). Boosting of cellular immunity against Mycobacterium tuberculosis and modulation of skin cytokine responses in healthy human volunteers by Mycobacterium bovis BCG substrain Moreau Rio de Janeiro oral vaccine. Infect. Immun. *74*, 2449–2452.

65. Hoft, D.F., Xia, M., Zhang, G.L., Blazevic, A., Tennant, J., Kaplan, C., Matuschak, G., Dube, T.J., Hill, H., Schlesinger, L.S., et al. (2018). PO and ID BCG vaccination in humans induce distinct mucosal and systemic immune responses and CD4(+) T cell transcriptomal molecular signatures. Mucosal Immunol. *11*, 486–495.

66. Folegatti, P.M., Ewer, K.J., Aley, P.K., Angus, B., Becker, S., Belij-Rammerstorfer, S., Bellamy, D., Bibi, S., Bittaye, M., Clutterbuck, E.A., et al.; Oxford COVID Vaccine Trial Group (2020). Safety and immunogenicity of the ChAdOx1 nCoV-19 vaccine against SARS-CoV-2: a preliminary report of a phase 1/2, single-blind, randomised controlled trial. Lancet *396*, 467–478.

67. R Core Team (2018). R: A Language and Environment for Statistical Computing (R Foundation for Statistical Computing).

STAR★METHODS

KEY RESOURCES TABLE

REAGENT or RESOURCE	SOURCE	IDENTIFIER
Antibodies		
anti-CD3 – AF700 (clone SP34-2)	BD Biosciences	Cat#: 557917; RRID: AB_396938
anti-CD4 – PerCP.Cy5.5 (clone L200)	BD Biosciences	Cat#: 552838; RRID: AB_394488
anti-CD8α – APC-H7 (clone SK1)	BD Biosciences	Cat#: 641400; RRID: AB_164536
anti-CD14 – BV421 (clone M5E2)	BD Biosciences	Cat#: 565283; RRID: AB_2739154
anti-CD20 – BV421 (clone 2H7)	Biolegend	Cat#: 302334; RRID: AB_10965543
anti-CD28 – ECD (clone CD28.2)	IOTest	Cat#: 6607111; RRID: AB_1575955
anti-CD45 – BV786 (clone D058-1283)	BD Biosciences	Cat#: 563861; RRID: AB_2738454
anti-CD45RA – PE-CF594 (clone 5H9)	BD Biosciences	Cat#: 565419; RRID: AB_2739229
anti-CD69 – APC (clone FN-50)	Biolegend	Cat#: 310910; RRID: AB_314845
anti-CD69 – BV785 (clone FN-50)	Biolegend	Cat#: 310932; RRID: AB_2563696
anti-CD95 – BV605 (clone DX2)	Biolegend	Cat#: 305628; RRID: AB_2563825
anti-CD103 – FITC (clone Ber-ACT8)	Biolegend	Cat#: 350204; RRID: AB_10639865
anti-CCR5 – APC-H7 (clone 3A9)	BD Biosciences	Cat#: 560748; RRID: AB_1937308
anti-CCR7 – BV650 (clone G043H7)	Biolegend	Cat#: 353234; RRID: AB_2563867
anti-CXCR3 – PE-Cy7 (clone G025H7)	Biolegend	Cat#: 353720; RRID: AB_11219383
anti-PD1 – BV510 (clone EH12.2H7)	Biolegend	Cat#: 329932; RRID: AB_2562256
anti-IFN-γ – BV711 (clone 4S.B3)	BD Biosciences	Cat#: 502540; RRID: AB_2563506
anti-IL-2 – AF488 (clone MQ1-17H12)	Biolegend	Cat#: 500314; RRID: AB_493368
anti-IL10 – PE (clone JES3-9D7)	Biolegend	Cat#: 501404; RRID: AB_315170
anti-IL-17A – PE-Cy7 (ebio64DEC17)	Biolegend	Cat#: 25-7179-42; RRID: AB_11063994
anti-IL-17A – BV605 (clone BL168)	Biolegend	Cat#: 512326; RRID: AB_2563887
anti-TNF-α – BV650 (clone Mab11)	BD Biosciences	Cat#: 502938; RRID: AB_2562741
VIVID – BV421	Thermofisher	Cat#: L34955
GolgiPlug	BD Biosciences	Cat#: 555029; RRID: AB_2869014
Cytofix/Cytoperm	BD Biosciences	Cat#: 554714; RRID: AB_2869014
Goat Anti-Human IgM(μ chain) Antibody, Alkaline Phosphatase (AP) Conugate, Affinity purified	Invitrogen	Cat#: A18838; RRID: AB_2535615
Goat Anti-Human IgA(α chain) Antibody, Alkaline Phosphatase (AP) Conugate, Affinity purified	Invitrogen	Cat#: A18784; RRID: AB_2535561
Anti-MONKEY IgG (gamma chain)(GOAT) Antibody Peroxidase Conjugated	Rockland Inc	Cat#: 617-103-012; RRID: AB_218715
IgA biotinylated detection Ab (MT57)	Mabtech	3860-4; RRID: AB_10736549
IgG biotinylated detection Ab (MT78)	Mabtech	3850-6; RRID: AB_10666158
IgM biotinylated detection Ab (MT22)	Mabtech	3880-6; RRID: NA
Bacterial and virus strains		
M. tuberculosis strain Erdman K01	BEI Resources	Cat#: NR-50781
BCG, strain Sofia (5×10^5 CFU/dose)	InterVax Ltd	Cat#: N/A
MTBVAC (5×10^5 CFU/dose)	Biofabri	Cat#: N/A
Chemicals, peptides, and recombinant proteins		
Lymphoprep™	Axis-Shield	Cat#: AXI-1114547
Perchloric acid	Sigma-Aldrich	Cat#: 244252-1L
Formaldehyde (16%)	Thermo Scientific	Cat#: 28906
p-Nitrophenyl Phosphate (p-NPP) Alkaline Phosphatase Substrate	Merck Millipore	Cat#: ES009-500mL

(*Continued on next page*)

Continued

REAGENT or RESOURCE	SOURCE	IDENTIFIER
Streptavidine-FITC	Biolegend	Cat#: 405202
TMB, ELISA substrate	MT Diagnostics	Cat#: SB04/B
TMB, ELISPOT substrate	Mabtech	Cat#: 3651-10
Critical commercial assays		
NHP specific IFN-gamma ELISPOT antibody pairs	U-CyTech	Cat#: 610-10
BOVIGAM™ Tuberculin PPD stimulating antigen, Bovine; Purified Protein Derivative (*M. bovis*)	Life Technol. NV	Cat#: 760060
BOVIGAM™ Tuberculin PPD stimulating antigen, Avian; Purified Protein Derivative (*M. avium*)	Life Technol. NV	Cat#: 760065
Milliplex NHP Cytokine Magnetic Bead Panel	Merck Millipore	Cat#: PRCYTOMAG −40K
Experimental models: organisms/strains		
purpose-bred *Macaca mulatta* (rhesus macaques); adult (> 4 years of age) males and females; Indian-genotype	BPRC	N/A
Software and algorithms		
Eli.Analyze (ELISPOT; v6.1)	A.EL.VIS GmbH	N/A
FACSDiva Software v 8.0.1 (BD LSRII)	BD Biosciences	SCR_001456
Flowjo software v 10	Treestar	SCR_000410
LEGENDplexTM Data Analysis Software (V8.0)	Biolegend/Vigene Tech	N/A
GraphPad Prism v 8.4.2	GraphPad Software	https://www.graphpad.com:443/
Other		
Old Tuberculin	Synbiotics, Inc	N/A
Mycobacterium Tuberculosis - tuberculine PPD for *in vitro* use; Purified Protein Derivative (*M.tuberculosis*)	AJ Vaccines	Cat#: 2391
M. tuberculosis strain HN878 Whole Cell Lysate	BEI Resources	Cat#: NR-14824

RESOURCE AVAILABILITY

Lead contact

Further information and requests for resources and reagents should be directed to and will be fulfilled by the Lead Contact, Frank Verreck (verreck@bprc.nl).

Materials availability

This study did not generate new unique reagents. However, any remaining biomaterials from this study can be made available and shipped at receiver's cost upon specific request to the Lead Contact, for which we require completion of a *Simple Letter Agreement for Transfer of Materials*.

Data and code availability

All data there is, are presented in this paper (including supplementals) and can be made available in different formats upon reasonable request. This study did not generate any unique code.

EXPERIMENTAL MODEL AND SUBJECT DETAILS

Ethics & Animal Handling

All housing and animal care procedures were performed at the Biomedical Primate Research Centre (BPRC) in Rijswijk, the Netherlands, and in compliance with European directive 2010/63/EU as well as the "Standard for Humane Care and Use of Laboratory Animals by Foreign Institutions" provided by the Department of Health and Human Services of the US National Institutes of Health (NIH, identification number A5539-01). BPRC is accredited by the American Association for Accreditation of Laboratory Animal Care (AAALAC). An ethical framework approval from the independent, central animal experiments authority in the Netherlands (in Dutch: Centrale Commissie Dierproeven, CCD) was in place, and before start the study plan was approved by BPRC's institutional animal welfare body (in Dutch: Instantie voor Dierwelzijn, IvD). The BCG and MTBVAC immunogenicity study was registered under CCD.009.D (while the *Mtb*-infection samples used for immunological cross-comparison, were taken from a study registered under CCD.009.C; see also further below).

Twelve female and twelve male Indian-type rhesus macaques (*Macaca mulatta*) were selected from BPRC's breeding colonies and stratified by gender, age, body weight and social indicators for pairwise housing into 4 groups of 6 animals. Treatment was randomly assigned to each group.

Selected animals were negative for prior exposure to mycobacteria, as assessed by tuberculin skin testing with Old Tuberculin (Synbiotics Corporation, San Diego, CA) and an IFNγ ELISPOT using Purified Protein Derivative (PPD) from *Mycobacterium bovis*, *Mycobacterium avium* (both Life Technologies NV) or *Mycobacterium tuberculosis* (AJ Vaccines, Copenhagen, Denmark) for *in vitro* recall stimulation of PBMC.

Animals were housed pairwise at biosafety level 3 throughout the experiment and provided with enrichment in the form of food and non-food items on a daily basis. Animal welfare was monitored daily. Animal weight was recorded prior to each blood collection event.

All animal handling and bio-sampling was performed under ketamine sedation (10 mg/kg, by intra-muscular injection). For endobronchial instillation ketamine sedation (5mg/kg) was supplemented with intramuscular medetomidine (0.04 mg/kg) and an analgesic applied to the larynx.

Eight weeks after vaccine administration animals reached study endpoint by protocol and were euthanized by intravenous injection of pentobarbital (200 mg/kg) under ketamine sedation. All animal care and veterinary personnel were blinded to experimental treatment.

Vaccines, Vaccine Preparation & Administration

Animals were vaccinated either with Bacillus Calmette Guérin strain Sofia (InterVax Ltd., Ontario) or with MTBVAC (Biofabri, Spain), and either via the skin or the pulmonary mucosa. The intradermally vaccinated groups received a standard, adult human dose of 1.5-6.0 x10^5 CFU BCG or 3.0-17.0 x10^5 CFU MTBVAC in 0.1 mL reconstituted vaccine in the skin (abbreviated as BCG.id or MVAC.id). The mucosally vaccinated groups were administered the same dose, but in 10 mL of sterile saline solution by endobronchial instillation into the lower right lung lobe (abbreviated as BCG.muc/B.muc or MTBVAC.muc/M.muc). The vaccines, regardless of administration route, were prepared from a single, pooled mix of freshly reconstituted vials, immediately prior to administration. Vaccination was executed for all animals in a single session in random order within 2-3 hours from vaccine preparation.

Mtb Infection

For the comparison of homing marker expression by cytokine positive pulmonary mucosal T cells, BALs from *Mtb* infected animals were obtained 11 weeks after endobronchial instillation of 3 to 15 CFU of *Mtb* Erdman (NR-50781, BEIResources). Infection was confirmed for all animals by the induction of *Mtb*-specific IFNγ production by PBMCs and by post-mortem pathology assessment (data not shown).

Biosample Collection & Processing

Cells from the pulmonary mucosa were recovered at specific time points by broncho-alveolar lavage (BAL), targeting either the lower right or lower left lung lobe. Three volumes of 20 mL of prewarmed 0.9% saline solution were consecutively instilled and recovered. BAL fluid was harvested by centrifugation of BAL samples for 10 minutes at 400 g after 100 μm filtration. Supernatant was subsequently decanted and stored at -80°C pending further analysis. The BAL cell pellet was taken up in RPMI supplemented with 10% fetal bovine serum (FBS), glutamax and penicillin/streptomycin (from hereon referred to as R10) and used in downstream assays. BAL fluid was filter-sterilized by centrifugation through 0.2 μm PVDF membrane plates (Fisher Scientific) before analysis.

Peripheral blood mononuclear cells (PBMC) were isolated from heparinised blood collected by venepuncture. Isolation of PBMCs was performed by density gradient centrifugation with Lymphoprep lymphocyte separation medium (Axis-Shield, UK), and PBMCs were subsequently resuspended in R10 for downstream immunological assays.

METHOD DETAILS

Flow cytometry

T cell cytokine production and homing marker expression was assessed by flow cytometry. Freshly isolated PBMC were incubated overnight with *Mtb* PPD (5 ug/mL) in the presence of GolgiPlug transport inhibitor (BD Biosciences). PMA/ionomycin stimulated samples were taken along as technical/positive controls. The next day, cells were washed and incubated with the panels listed in the Key Resources Table. To facilitate intracellular cytokine staining, cells were permeabilized with Cytofix/Cytoperm (BD Biosciences) before addition of cytokine antibodies. After overnight fixation with 2% paraformaldehyde,[66] samples were acquired on a 3-laser, 14-color LSR-II flow cytometer (BD Biosciences). Analyses were performed in FlowJo version 10 (Treestar). T cells were selected as Singlets/Lymphocytes/Viable/CD14-CD20-/CD45+/CD3+ events, after which further CD4 and CD8 gating was applied. Any anomalies indicative of unstable signal acquisition were excluded using the "Time" parameter. Cytokine positivity was determined by placement of cytokine gates on the medium control samples and subsequently applying the gates to the corresponding PPD stimulated samples.

Luminex

Cytokine production by BAL cells stimulated for 72 hours with PPD (5 ug/mL, final concentration), was assessed by customised Milliplex Luminex kits (Merck Millipore, USA). Assays were performed according to manufacturer's protocol. In short: supernatants of

stimulated BAL cells were incubated with beads coated with cytokine-specific antibodies. Bound cytokines were visualized using biotin-coupled detector antibodies and PE-labeled streptavidin. Beads were acquired on a Bioplex 200 system and cytokine levels were calculated with Bioplex Manager software version 6.1 (both Biorad, CA, USA).

IFNγ ELISPOT

Non-human primate specific IFNγ ELISPOT (U-CyTech, the Netherlands) was performed on PBMC according to manufacturer's protocol on. Briefly, 200,000 PBMC were incubated in triplicate for 24 hours with *Mtb*-derived PPD (AJ Vaccines, Denmark) or recombinant ESAT6-CFP10 fusion protein (provided by Kees Franken from the Ottenhoff lab, Leiden University Medical Centre). The next day cells were washed and transferred to anti-IFNγ coated membrane plates (Millipore). After 24 hours, cells were discarded and membrane-bound IFNγ was visualized using a biotinylated anti-IFNγ detector antibody, streptavidin-horseradish peroxidase conjugate and tetramethylbenzidine substrate. Spots were quantified using an automated reader (AELVIS, Hannover).

Immunoglobulin ELISA

Antibody levels in BAL were determined by Enzyme Linked ImmunoSorbent Assay (ELISA). In brief, 96-well plates were coated with either 5 μg/mL *Mtb* strain HN828 Whole Cell lysate (BEI Resources, VA, USA) in PBS. After overnight blocking with 1% BSA, samples were added to the wells. Bound antibodies were subsequently detected either with horse radish peroxidase-conjugated anti-IgG (Rockland, PA, USA), alkaline phosphatase-conjugated anti-IgA (Fisher Scientific) or alkaline phosphatase-conjugated IgM (Sigma), and the subsequent addition of para-nitrophenylphosphate substrate for ELISA color development. All samples were normalized to arbitrary units (AU) against a serial dilution of a positive reference sample included in all assays.

Mtb binding and phagocytosis assay

To assess *Mtb* binding of immunoglobulins, 0.05 mL aliquots of BAL fluid obtained prior to and 8 weeks after vaccination, were incubated at 37°C for 1 hour with 10^7 CFU of *Mtb* H37Rv-dsRed. (Korbee et al., 2018) Subsequently, samples were equally divided over three vials and biotinylated detection antibodies specific for IgA, IgG or IgM (all from Mabtech) were added (final dilution 1:500). After 30 minutes of incubation at room temperature, streptavidin-FITC (final dilution 1:400) was added, and samples were incubated for a further 60 minutes toward detection of bound antibody. Samples were fixed overnight with 2% PFA before analysis.

For the phagocytosis assay, $5x10^5$ THP1 cells were seeded in a 24-wells plate and activated by overnight incubation with 10ng/mL PMA at 37°C. The next day, 10^7 CFU of *Mtb* H37Rv-GFP was incubated with BAL fluid as described above, and subsequently added to the activated THP-1 cells. After 4 hours cells were dissociated with trypsin-EDTA and resuspended in 2% PFA for overnight fixation. The binding assay samples were subsequently acquired on a 4 laser, FACSAriaIII system; samples from the phagocytosis assay were acquired on a 3 laser, Beckman Coulter Gallios system. For both assays, *Mtb* H37Rv-dsRed or -GFP incubated in PBS only was taken along as a negative control.

QUANTIFICATION AND STATISTICAL ANALYSIS

Statistical analysis was performed with Graphpad Prism version 8 and R version 3.5.1.[67] Significance of differences between groups was calculated by two-sided Mann-Whitney testing of which Holm's adjusted p values are reported. Correlation statistics were generated by Spearman's rank analysis.

Cell Reports Medicine, Volume *2*

Supplemental Information

Pulmonary MTBVAC vaccination induces immune signatures previously correlated with prevention of tuberculosis infection

Karin Dijkman, Nacho Aguilo, Charelle Boot, Sam O. Hofman, Claudia C. Sombroek, Richard A.W. Vervenne, Clemens H.M. Kocken, Dessislava Marinova, Jelle Thole, Esteban Rodríguez, Michel P.M. Vierboom, Krista G. Haanstra, Eugenia Puentes, Carlos Martin, and Frank A.W. Verreck

Supplemental Figure 1: Serum C-reactive protein levels post vaccination (*Relating to Figure 1*)

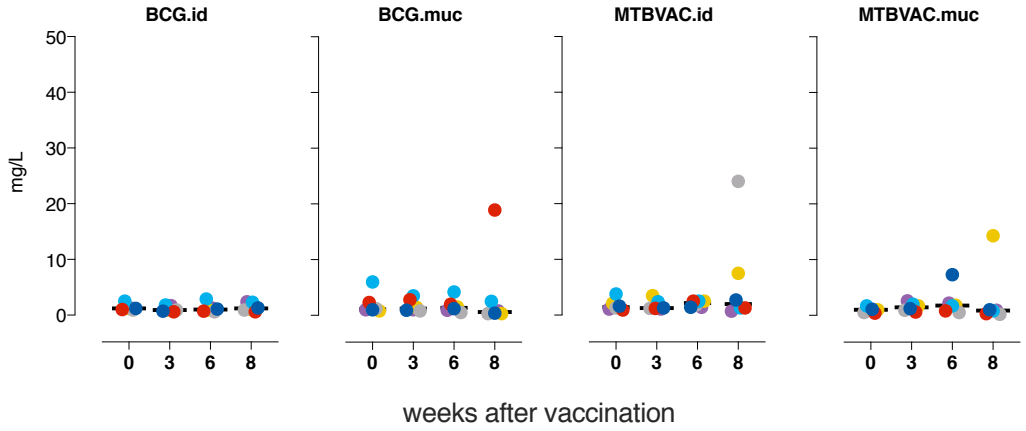

Levels of C-reactive protein did not reveal any adverse systemic inflammatory response after vaccination. Individual CRP values are plotted per treatment group over time, with horizontal bars indicating medians.

Supplemental Figure 2: BAL CD8+ T-cell responses and proliferation, and bronchoalveolar lymph node CD4+ T-cell responses (*Relating to Figure 2*)

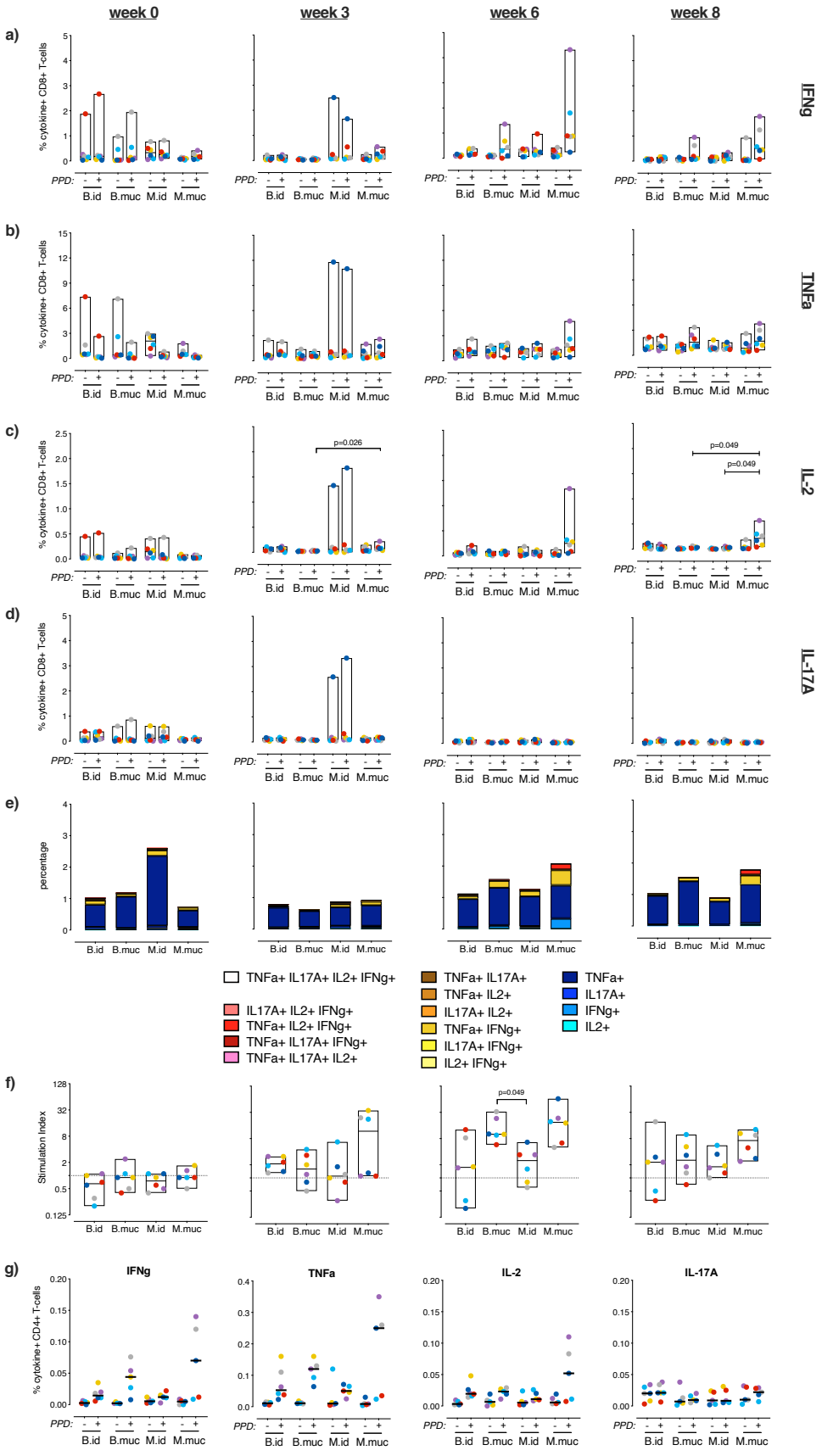

Flow cytometric analysis of **a)** IFNγ, **b)** TNFα, **c)** IL2 and **d)** IL17A responses in CD8+ T-cells before and at various time points after vaccination, either or not upon *vitro recall* stimulation with PPD. **e)** Stacked bar graphs depicting frequencies of single and multiple cytokine producing subsets of CD8+ T-cells after PPD stimulation by median values. **f)** PPD-specific proliferation of BAL cells, depicted as the stimulation index: the ratio of antigen- over medium control-stimulated values. **g)** Production of IFNγ, TNFα, IL2 and IL17A by CD4+ T-cells from lung draining lymph nodes either or not in response to PPD, 8 weeks after vaccination.

In **a-d** and **g** "+" indicates PPD stimulated samples; "-" indicates unstimulated, culture medium-incubated samples as controls. For all graphs n=6 animals per group. Horizontal lines in bars indicate group medians. Significance of group differences was determined by two-sided Mann-Whitney test adjusted for multiple comparisons. Holms adjusted p-values ≤ 0.05 are depicted. Colour coding per individual is consistent throughout the paper including supplementals.

Supplemental Figure 3: Cytokine production by peripheral CD4+ T-cells (*Relating to Figure 3*)

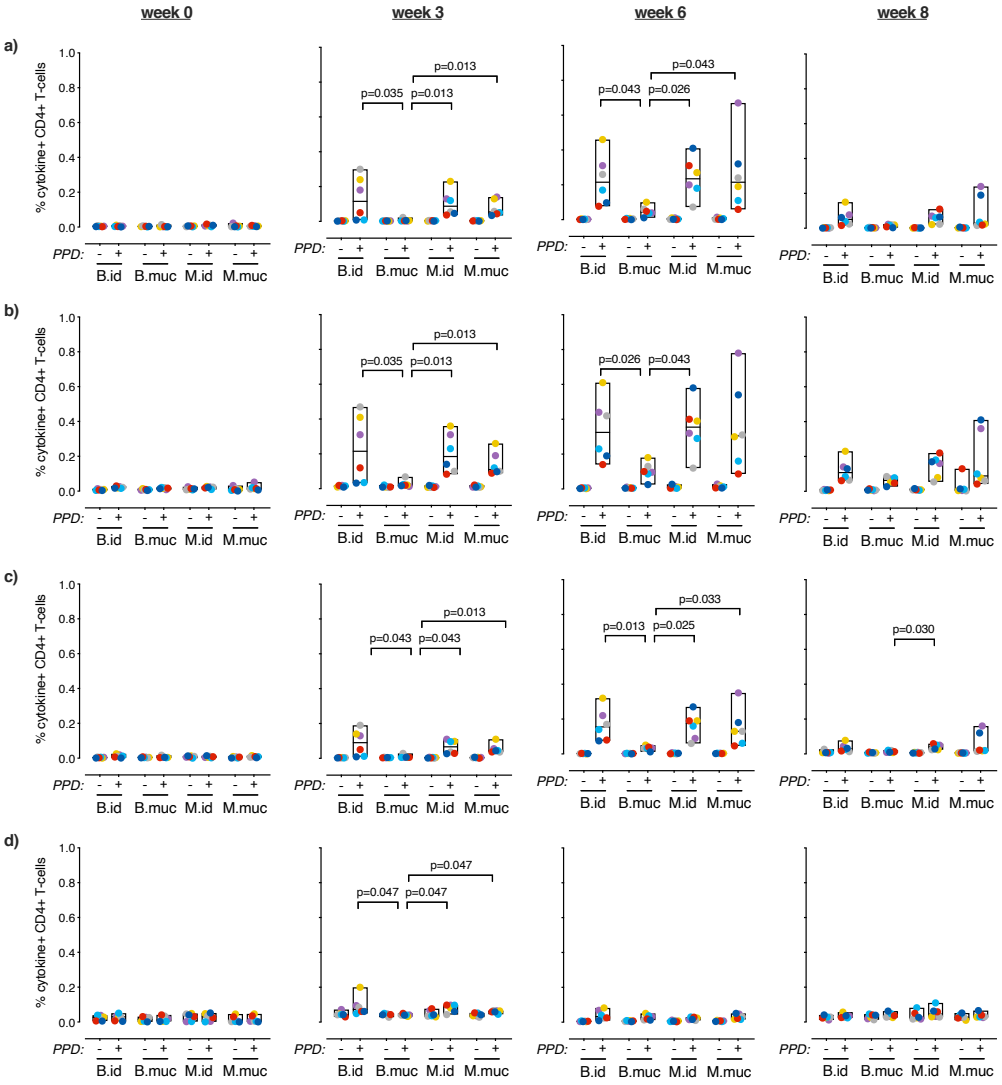

Production of **a)** IFNγ, **b)** TNFα, **c)** IL2 and **d)** IL17A by peripheral CD4+ T-cells before and at various time points after vaccination, either or not upon *in vitro* recall stimulation with PPD.

PPD stimulated samples are indicated by "+", "-" indicates unstimulated, culture medium control samples. For all graphs n=6 animals per group. Horizontal lines indicate group medians. Significance of group differences was determined by two-sided Mann-Whitney test adjusted for multiple comparisons. Holms adjusted p-values ≤ 0.05 are depicted. Colour coding per individual is consistent throughout.

Supplemental Figure 4: Cytokine production by peripheral CD8+ T-cells (*Relating to Figure 3*)

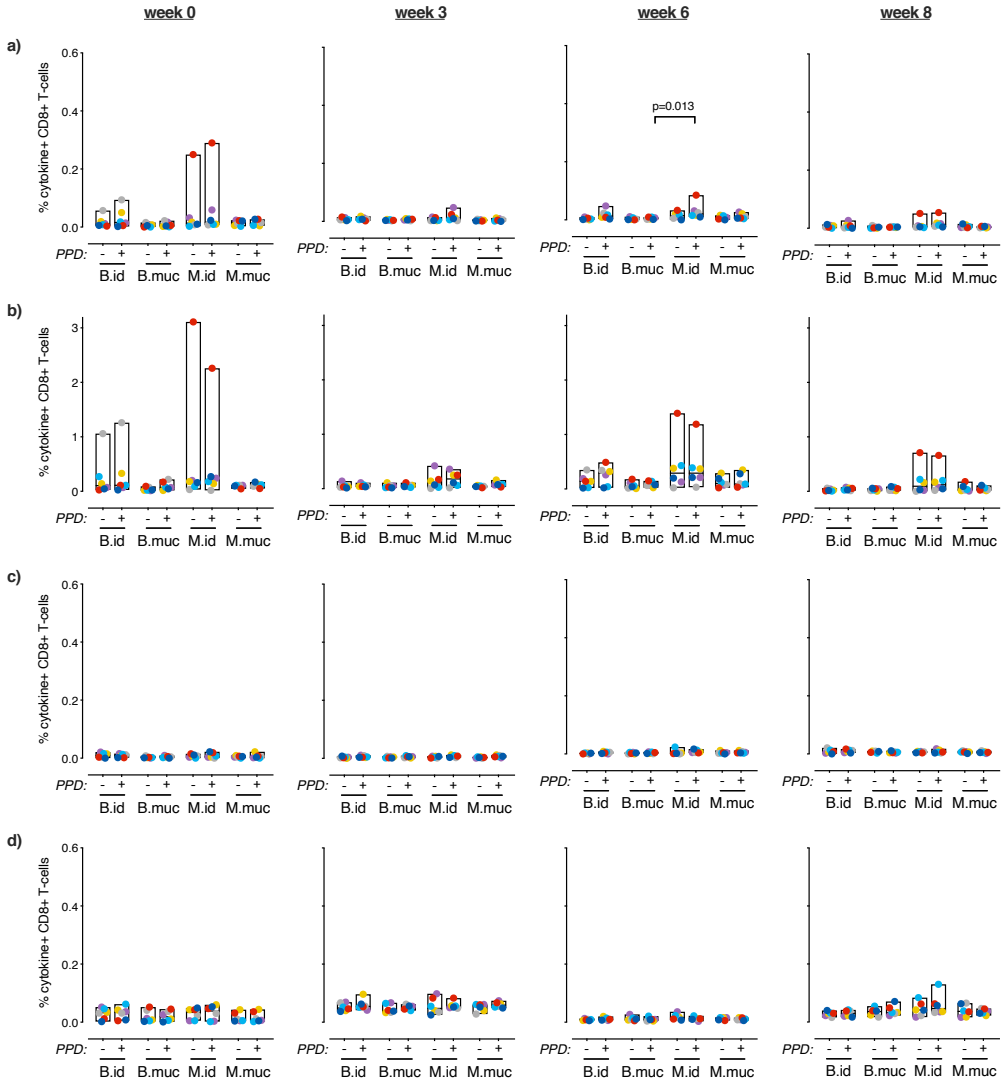

Production of **a)** IFNγ, **b)** TNFα, **c)** IL2 and **d)** IL17A by peripheral CD8+ T-cells before and at various time points after vaccination, either or not upon *in vitro* recall stimulation with PPD.

PPD stimulated samples are indicated by "+", "-" indicates unstimulated, culture medium control samples. For all graphs n=6 animals per group. Horizontal lines indicate group medians. Significance of group differences was determined by two-sided Mann-Whitney test adjusted for multiple comparisons. Holms adjusted p-values ≤ 0.05 are depicted. Colour coding per individual is consistent throughout.

Supplemental Figure 5: Cytokine production by CD4+ T-cells in TST-DTH draining lymph nodes (*Relating to Figure 3*)

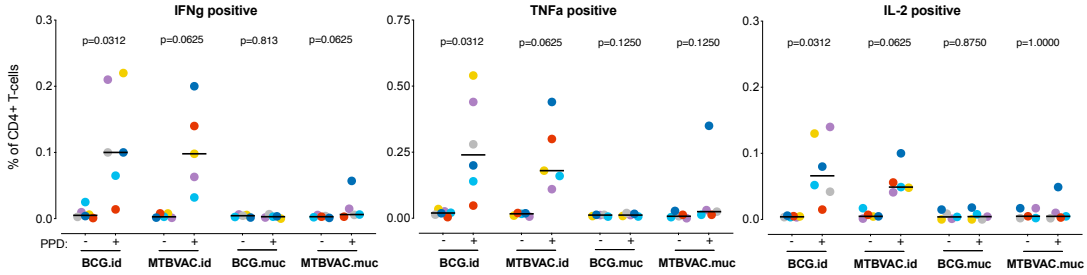

Production of IFNγ, TNFα, and IL2 by CD4+ T-cells in axillar lymph nodes draining the injection site of the diagnostic Tuberculin Skin Test (TST), which was applied at week 8 after vaccination to investigate if mucosal vaccine routing would result in a distinctive T-cell response after *in vivo* recall stimulation.

For all graphs n=5 animals per group, except for BCG.id (n=6). Horizontal lines indicate group medians. Significance of antigen-specific responses was determined by Wilcoxon matched pairs-signed rank testing. Colour coding per individual is consistent throughout.

Supplemental Figure 6: Homing marker expression by peripheral T-cells (*Relating to Figure 4*)

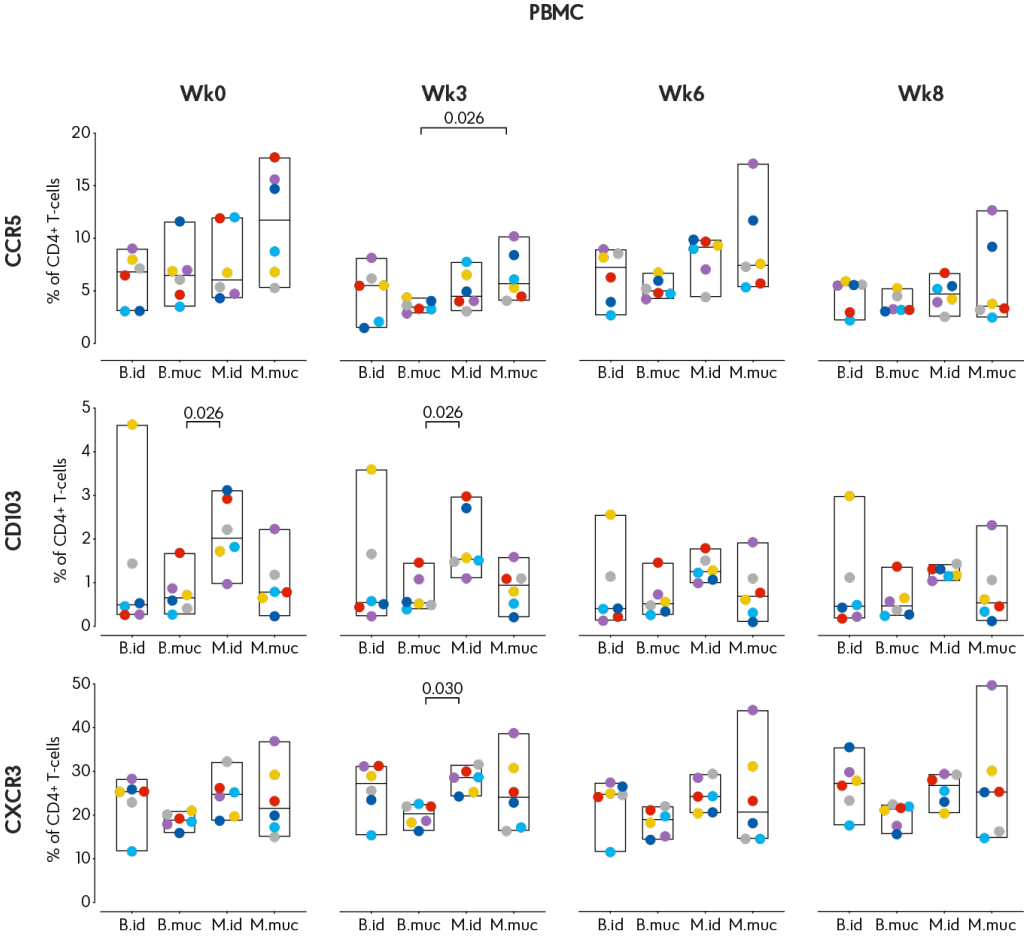

Frequency of CCR5+, CD103+ and CXCR3+ CD4+ T-cells in unstimulated peripheral blood mononuclear cells before and at various time points after vaccination.

For all graphs n=6 animals per group. Horizontal lines indicate group medians. Significance of group differences was determined by two-sided Mann-Whitney test adjusted for multiple comparisons. Holms adjusted p-values ≤ 0.05 are depicted. Colour coding per individual is consistent throughout.